Journal of

RESIDUALS
SCIENCE
& TECHNOLOGY

Contents

Aim and Scope

The objective of the *Journal of Residuals Science & Technology* (JRS&T) is to provide a forum for technical research on the management and disposal of residuals from pollution control activities. The Journal publishes papers that examine the characteristics, effects, and management principles of various residuals from such sources as wastewater treatment, water treatment, air pollution control, hazardous waste treatment, solid waste, industrial waste treatment, and other pollution control activities. Papers on health and the environmental effects of residuals production, management, and disposal are also welcome.

Editor-in-Chief

P. Brent Duncan
Department of Biology
University of North Texas
Denton, TX, USA
pduncan@unt.edu

Editorial Advisory Board

C O N T E N T S

Research

R E S E A R C H

Determination of Optimum Polymer Dose using UV-vis Spectrophotometry and its Comparison to Filtration Based Tests

SAMAN AGHAMIR-BAHA and BANU ÖRMECI

Department of Civil and Environmental Engineering, Carleton University, 1125 Colonel By Drive, Ottawa, ON K1S 5B6, Canada

ABSTRACT: In this study, residual polymer concentration in sludge filtrate was measured by measuring the absorbance of samples at 190 nm. In addition, the method was used to determine the optimum polymer dose required to condition sludge. The optimum dose determined by the UV-vis method was compared to the optimum doses determined by the capillary suction time (CST) and filtration tests. The results showed the UV-vis method was in close agreement with the CST and filtration tests in determining the optimum polymer dose. The advantage of the UV-vis method over other methods is that it can be used in-line at wastewater treatment plants for monitoring and optimizing polymer dose.

INTRODUCTION

THE ease at which sludge is dewatered is mainly a function of polymer dose during conditioning phase; there is an optimum polymer dose that results in the most water release from sludge solids, above and below which dewatering is worsened. Dewatering performance also changes by variations in factors such as duration and intensity of mixing.

Due to the continuous changes in the wastewater characteristics and related treatment processes, sludge characteristics also change on a continuous basis. Changes in sludge characteristics require frequent adjustments to the optimum polymer dose that results in the most water release from sludge. To ensure that the polymer dosed to sludge is at the optimum dose, jar test experiments need to be performed by the treatment plant personnel.

The difficulty with such tests is that they do not quantify a fundamentally based physical parameter of sludge, nor they can be easily employed for dewatering optimization, and predict the efficiency of a full-scale dewatering device [1]. Moreover, performing such tests, requires involvement of a highly skilled operator, and fails to produce real-time results; as they are time-consuming, and by the time the results are available, they might not be applicable, due to the constant changes in sludge characteristics. There is therefore the

need for methods that can measure optimum polymer dose in-line, and make corresponding adjustments to concentration of polymer being added to sludge in real-time.

Some of the methods that were previously suggested for in-line polymer dose optimization include streaming current detector [2,3], centrate viscosity [4], and torque rheology [5,6,7].

In-line and real-time methods would be further practical if they could directly measure the concentration of residual polymer in filtrate or centrate and use that information towards adjusting the concentration of polymer being added to sludge. However, monitoring the concentration of polymers in the filtrate is a formidable task not well suited to industrial applications as analytical techniques for this purpose are complicated and time consuming and do not permit real-time results. Electronic instrumentation to determine electric charge is available, but such devices are expensive, and do not differentiate between charge associated with a polymer, or charge from other sources, including the water, solids, or other constituents in the effluent [8].

Nevertheless, Budd *et al.* [8] developed a method for controlled addition of polymer in water treatment plants based on direct measurements of residual polymer concentration to produce water with low solids contents for utilization in industry. For this purpose, depending on the concentration of polymer being added to untreated water, a fluorescing molecule, with an opposite charge to that of polymer was also added. The

*Author to whom correspondence should be addressed.
E-mail: banu_ormeci@carleton.ca

oppositely charged polymer and fluorescing molecule then produced a complex that could be used to monitor the concentration of polymer in the effluent. The concentration of polymer being added to water could then be adjusted based on the concentration of polymer-fluorescing complex in the effluent using a control loop. This method was the first attempt to directly measure the residual polymer concentration. However, the need for introduction of an external fluorescing molecule to water and potential consumption of the fluorescing molecule with other water constituents limited the application of the method.

UV-Vis spectroscopy has recently emerged as a new method for detection of polymers used in water and wastewater treatment [9,10,11]. It was reported that polyacrylamide polymers strongly absorb light at around 190 nm and the absorbance is directly proportional to the polymer concentration. The goal of this study was to determine whether the UV-Vis method could successfully be used for the detection of residual polymer in sludge filtrate after dewatering, and whether a relationship could be established between the residual polymer concentration in filtrate and the optimum polymer dose. If successful, the UV-Vis method could potentially be used in-line and real-time at treatment plants in the future to achieve optimization of polymer dose and sludge dewatering. UV-Vis spectroscopy is especially suitable for this, as in-line spectrophotometers are already used at water treatment plants for detection of organic matter and full-scale in-line instruments are available in the market.

MATERIALS AND METHODS

Polymer Stock Solution

Polymer stock solutions of 5 g/L or 0.5% were prepared as follows: in three plastic weighing dishes, 5 g of Zetag8160 (polyacrylamide, medium-high cationic charge, high molecular weight, granular solid form), 5 g of SNF475 (polyacrylamide, high charge density, ultra-high molecular weight, granular solid form), and 5 g of CIBA (polyacrylamide, high charge density, high molecular weight, free-flowing microbead) were weighted using a scale (SI-114, Denver Instruments, Canada), and decanted into three 1 L glass beakers. The beakers were then diluted with deionized water up to a volume of 1 L. Using a jar tester (Phipps and Bird, USA), the mixtures were then stirred at 300 rpm for 5 minutes followed by 55 minutes at 250 rpm and were allowed to rest for 60 minutes prior to usage.

Dewatering Experiments

Anaerobically digested sludge from the Ottawa Wastewater Treatment Plant (ROPEC) was collected and was mixed at 200 rpm for two minutes and 30 seconds using a jar tester. A minimum of five different polymer concentrations was used for conditioning sludge. The polymers used for dewatering tests included Zetag8160, SNF475 and CIBA.

Capillary Suction Time (Type 319 multi-CST, Triton Electronics, Canada) and filtration tests were used as indicators to monitor the filterability of conditioned sludge samples. Three replicates were used for the CST test.

For filtration tests, 200 mL of the conditioned sludge samples was poured in the funnel of the filtration apparatus, using a medium-flow filter paper (#P5, Fisher Scientific, Canada). A time of about 3 minutes was allowed for filtration and the final volume of the collected filtrate was recorded for each sample.

The filtrate from the filtration tests was then diluted at a ratio of 1v (filtrate): 9v (deionized water). The absorbance of the diluted samples was measured using a UV-Vis Spectrophotometer (Cary 100 Bio UV-Vis Spectrophotometer, Varian Inc./Agilent Technologies, Canada) and was recorded at a range of 190–300 nm using the Scan software (Cary WinUV, Varian Inc., Canada).

RESULTS AND DISCUSSION

Capillary Suction Time (CST)

CST is the time the liquid fraction of the conditioned sludge takes to travel 1 cm radially. CST has its lowest value at around the optimum dose and increases in the under dose and over dose polymer range producing a U shaped curve. Figures 1 through 3 demonstrate the
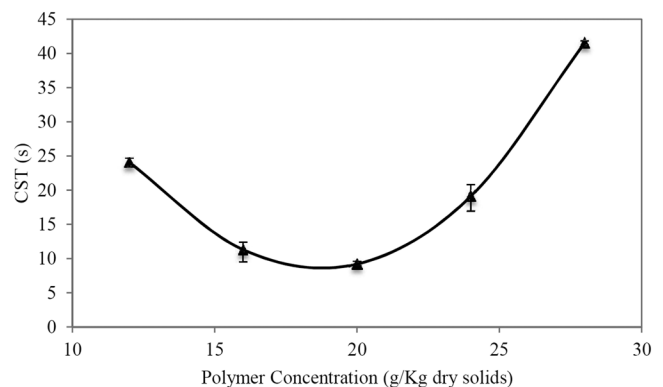

Figure 1. *CST test results from Zetag 8160 (average of three measurements).*
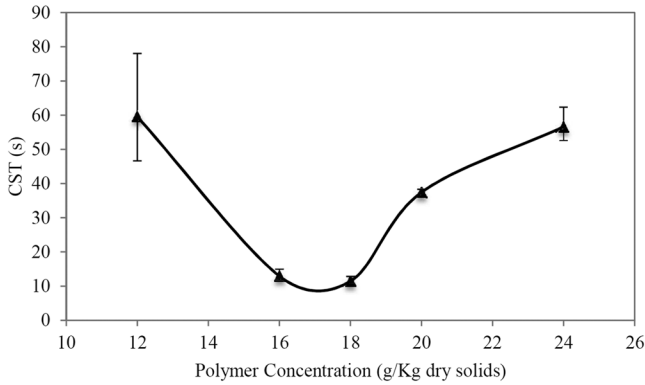
Figure 2. *CST test results from SNF475 (average of three measurements).*

Figure 4. *Filtration test results from Zetag8160.*

change in CST values of anaerobically digested sludge as the dosage of conditioner is changed for the three polymers of Zetag8160, SNF475, and CIBA, respectively. The expected U shape trend is clearly evident with all of the different polymers used.

As expected, the optimum polymer dosages are different between the three different polymers varying from 15–20 g polymer/Kg dry solids, with CIBA having the lowest and Zetag8160 having the highest optimum dose. The differences in the polymer doses can be explained by the differences in the chemistry of polymer and their compatibility with the characteristics of the sludge used.

Filtration Tests

Filtrate volume is highest at the optimum polymer dose. As polymer dose increases, an increase in the amount of filtrate is expected until the optimum point is reached after which, further increase in polymer, results in reduction in filtrate volume. This provides the shape of an upside down U for the plot of filtrate volume versus polymer concentration.

Figures 4 through 6 show the curves for volume of filtered sludge water as concentration of polymers of Zetag8160, SNF475, and CIBA are increased. The optimum dose associated with the three polymers ranged from 17–20 g polymer/Kg dry solids with CIBA polymer having the lowest optimum dose, and Zetag8160 polymer having the highest. The same trend was observed for CST tests of the three polymers.

For the polymers of Zetag8160 and SNF475, the CST and filtration tests agree on the same polymer dose to be the optimum. For the CIBA polymer, the CST test shows the optimum dose to be 15 g polymer/Kg dry solids whereas in the filtration test, a sludge sample containing 17.5 g polymer/Kg dry solids appears to have the highest volume of filtrate produced. This is likely because the sub-samples taken for CST and filtration tests from mother-sample differed in terms of the solid/liquid content. In other words, since these samples were poured from a larger conditioned and flocculated mother sample, there is a high chance that the solid and liquid proportions were not equal for different sub-samples. Therefore, some variation in results between different sub-samples taken for CST and filtration tests could be expected.

Figure 3. *CST test results from CIBA (average of three measurements).*
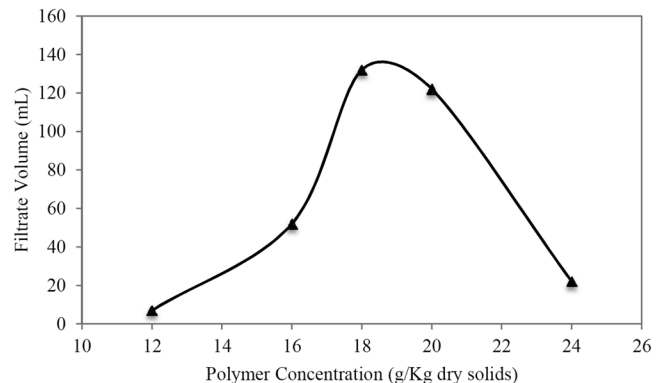
Figure 5. *Filtration test results from SNF475.*
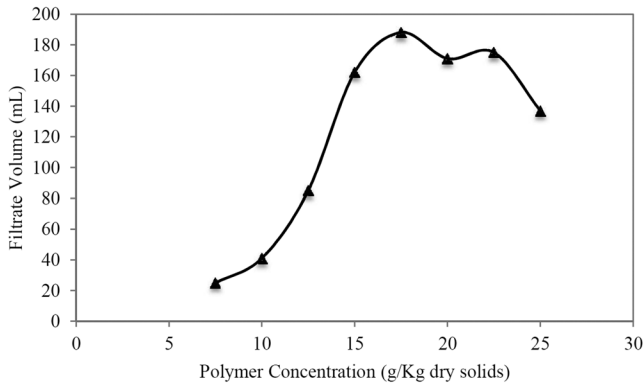
Figure 6. *Filtration test results from CIBA.*

Figure 8. *Filtrate absorbance at 190 nm with SNF475 (average of three measurements).*

Absorbance Method

The absorbance spectra of diluted filtrate samples were measured at 190 nm, which was reported to be in the wavelength range where peak absorbance is observed for polyacrylamide polymers (Gibbonsand Örmeci, 2013 and Al Momani and Örmeci, 2014). Figure 7 shows the absorbance values of Zetag8160 plotted against polymer concentration. The same measurements for SNF475 polymer are provided in Figure 8, and for CIBA polymer in Figure 9, respectively.

As shown in Figures 7, 8, and 9, as the concentration of polymers are increased, the absorbance of filtrate decreases up to a point, after which, further increase in polymer concentration results in an increase in the filtrate absorbance. This trend is very similar to what would be expected from a conventional filterability test such as CST.

This absorbance behavior of filtrate at $\lambda = 190$ nm could be explained by the fact that as polymer dose increases, smaller particles are removed from filtrate and are incorporated in the flocs, the filtrate gets purer

and this results in a decrease in the absorbance of filtrate. This trend continues until the optimum dose is reached. Beyond the optimum point, the extra polymer associates in the liquid (filtrate) phase directly due to the lack of new sludge surfaces to react with, and therefore increases the absorbance of the filtrate at 190 nm. Consequently, the absorbance of the filtrate exhibits a U shaped curve and the minimum absorbance corresponds to the optimum polymer dose.

In Figure 7, the increase in filtrate absorbance in the over-dosing region is clearly evident. However in Figures 8, and 9 this increase is not as steep as Figure 8, and instead of having one point corresponding to a minimum absorbance value, the plots exhibit a minimum plateau. This is likely due to the low dilution ratio that was used to dilute the filtrate samples. The measured absorbance values are on the high side and exceed the ideal detection range (0–1 AU) of the instrument, which results in loosing the sensitivity of the measurements. Nonetheless, the first point in the plateau (minimum region) corresponds to the optimum dose for SNF475, and CIBA polymers.

Based on the explanation given above, the optimum

Figure 7. *Filtrate absorbance at 190 nm with Zetag8160 (average of three measurements).*
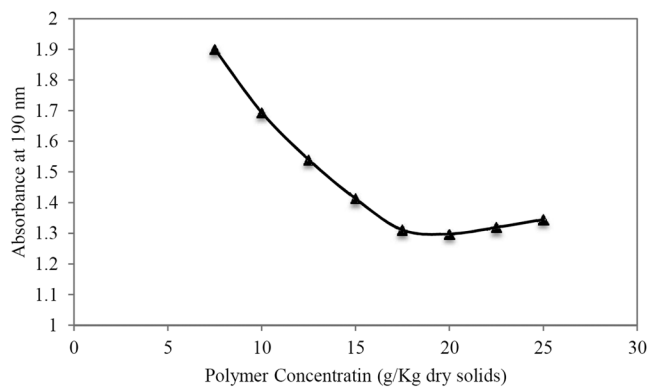
Figure 9. *Filtrate absorbance at 190 nm with CIBA (average of three measurements).*

dose for Zetag8160, and SNF475 polymer appears to be 20 g/Kg dry solids, whereas for CIBA polymer it is 17.5 g/Kg dry solids.

Comparison of Optimum Doses

The purpose of running CST and filtration tests in this chapter was to determine whether the optimum polymer dose specified by UV-Vis spectroscopy would be in agreement with the optimum doses determined by the conventional filterability tests. The optimum doses approximated by each method and for each polymer are provided in Table 1.

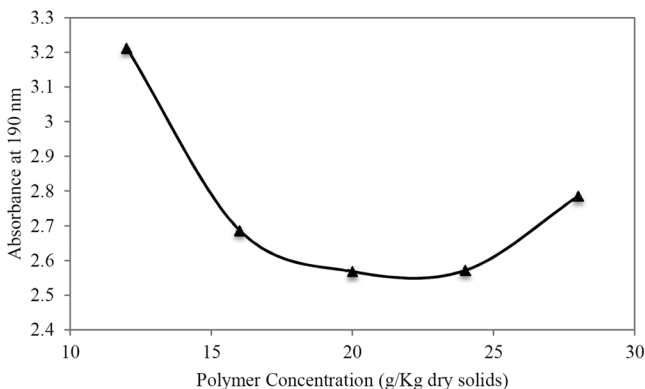As demonstrated in Table 1, for two out of the three polymers assessed, the result from absorbance method either agreed with the result of one (CIBA) or both tests (Zetag8160), and for SNF475 polymer there was a close agreement between the optimum doses determined by absorbance test to that of CST, and filtration tests. The differences could be explained by the differences in samples, different structures of polymers as well as the chosen incremental increases in polymer during jar tests.

Use of Absorbance Method as an In-Line Method

The results illustrated herein indicate that the UV-Vis absorbance method can be used for the detection and quantification of residual polymer in filtrate after sludge dewatering, and also for the determination of the optimum polymer dose required to condition sludge. A control loop such as the one presented in Fig-

Table 1. Optimum Doses for All Polymers Determined by All Methods.

Polymers	Optimum Dose for: (g/Kg dry solids)		
	CST	Filtration Test	Absorbance Test
Zetag8160	20	20	20
SNF475	18	18	20
CIBA	15	17.5	17.5

ure 10 can be used in an automated system to identify the optimum polymer dose in-line and make frequent adjustments in polymer dosage being added to sludge in real-time. UV-Vis spectroscopy is especially suitable for this purpose, since there is no need for chemical reagents.

CONCLUSIONS

A new UV-Vis based method was used for detection of residual polymer concentration in filtrate after sludge dewatering and identification of optimum polymer dose required to condition sludge. The optimum polymer dose was also identified using well-established CST and filtration tests. For the three different polymers assessed, the results from UV-Vis based method were in close agreement with the CST and filtration tests. One of the advantages of the UV-vis method is that it can be used in-line at wastewater treatment plants to generate real-time information on polymer dosing. As the next step, the method should be tested at a full-scale treatment plant to confirm the results of this study at the full-scale.
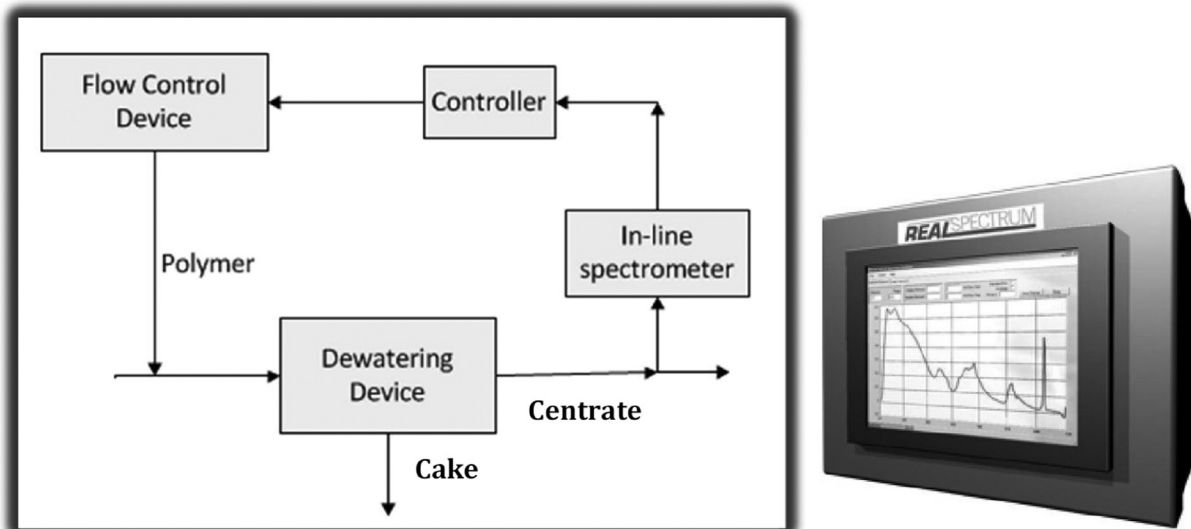
Figure 10. Example of a control loop for automatic adjustments in dosage of polymer being added to sludge using an in-line UV-vis spectrophotometer.

REFERENCES

1. Dentel, Steven K. Evaluation and role of rheological properties in sludge managements. *Journal of Water Science Technology,* 1997: 662–668.

2. Dentel, S. K. and Abu-Orf, M. M. Laboratory and full-scale studies of liquid stream viscosity and streaming current for characterization and monitoring of dewaterability. *Water Research, 29* (12), 1995, 2663–2672.

3. Abu-Orf, M. M. and Dentel, S. K. Automatoc control of polymer dose using the streaming current detector. *Water Environment Research, 70* (5), 1998, 1005–1018.

4. Bache, D. H. and Papavasilopoulos, E. N. (2000) Viscous behavior of sludge centrate in response to polymer conditioning. *Water Research, 34* (1), 354–358.

5. Campbell, Herbert W., and Phillip J. Crescuolo. Process and apparatus for controlled addition of conditioning material to sewage sludge. US Patent US4544489 A. 1985.

6. Abu-Orf, M. M. and Örmeci, B. Measuring sludge network strength using rheology and relation to dewaterability, filtration and thickening—Laboratory and full-scale experiments. *Journal of Environmental Engineering, 131* (8), 2005, 1139–1146.

7. Örmeci, B. Optimization of a full-scale dewatering operation based on the rheological characteristics of wastewater sludge. *Water Research, 41* (6), 2007, 1243–1252.

8. Budd, Scott S., Narasimha M. Rao, Jitendra Shah, and Ananthasubra Sivakumar. Fluorescent tracer in a water treatment process. USA Patent US5413719 A., 1995.

9. Gibbons, Meaghan, and Banu Örmeci. Quantification of polymer concentration in water using UV-Vis spectroscopy. *Journal of Water Supply: Research & Technology-AQUA 62*, no. 4 (2013): 205–213.

10. Al Momani F. and Örmeci B. In-line and real-time measurement of polymer concentration in water and wastewater. *Journal of Chemical Engineering Journal*, 2014, *2* (2), 765–772.

11. Al Momani, F. and Ormeci, B. (2014) Optimization of Polymer Dose Based on Residual Polymer Concentration in Dewatering Supernatant. *Water, Air, & Soil Pollution*, in print.

Co-Digesting Sewage Sludge Using Rice Straw and Effective Microorganisms (EM1)

E. RASHED[1], A. HASSAN[2] and L. AHMED[2,*]

[1]Sanitary Engineering Department, Faculty of Engineering, Cairo University
[2]Sanitary Engineering Departments, National Housing and Building Research Center

ABSTRACT: Anaerobic digestion is a solution for sludge management. It is organic matter converted into methane which is renewable energy. This energy is used to enhance performance of co-digestion of sewage sludge using rice straw and effective microorganisms (EM1). A study using a bench scale was installed at El-Berka waste water treatment plant (WWTP) in the El-Salam district, Cairo, Egypt with mesophillic conditions for thickened sludge. The bench scale was monitored for three stages over 20 days of operation to choose the most suitable rate of rice straw and EM1 mixed with thickened sludge. It was concluded that 20% rice straw and 1:250 EM1 mixing rate was the most suitable ratio based on COD and total VSS destruction percentage. Results showed a reduction of COD and total VSS up to 70 and 77%, respectively.

INTRODUCTION

THE purpose of treating wastewater is to remove impurities and to consolidate it into a smaller volume of liquid. The objective of processing sludge in this manner is to extract its water from solids and dispose of the de-watered residue (i.e., the solids). Concentration of organic matter in wastewater may be within 200 mg/l while that in a typical sludge could be within 40,000 mg/l. Thus, treatment of 1 million m^3 of wastewater produces about 5,000 m^3 of sludge [1]. Quantities and nature of sludge relates to characteristics of raw wastewater and selected processing methods.

Sewage sludge, a product of wastewater treatment, is rich in nutrients and trace elements and may be reused in agriculture as a fertilizer and soil conditioner. High odor emission, high levels of heavy metals and toxic organic compounds, and presence of potentially pathogenic microorganisms demand pretreatment of sewage sludge before agricultural related application [2].

A major problem facing municipalities throughout the world is the treatment, disposal, and/or recycling of sewage sludge [3]. For many years the methods and technologies for sewage sludge treatment which are implemented in Egypt were very limited. The main focus was devoted to the process of sludge drying mainly through natural drying beds without any interest related to the characteristics or quality of sludge produced. Recently, there is an interest in expanding the use of new techniques and methods for sewage sludge treatment.

The existing wastewater treatment plants in Egypt produce an estimated quantity of dry sludge of 950,000 tons per year and are expected to increase to 2 million tons/yr by 2020. Various treatment techniques are employed for sludge. Presently in Cairo at a wastewater treatment plant in the east bank area, produced sludge is treated in temporary drying beds [4].

The handling of sewage sludge is one of the most significant challenges in wastewater management. In many countries sewage sludge is a serious problem due to high treatment costs and risks to environment and human health. Although, the volume of produced sewage sludge represents only 1–2% of treated wastewater volume, its management costs usually range from 20% to 60% of total operating costs for the wastewater treatment plant [5].

Anaerobic digestion is an interesting solution to the wastewater sludge management issue. Objectives of anaerobic digestion are stabilization of organic solids, sludge volume reduction, odor reduction, and destruction of pathogenic organisms, useful gas production, and improvement of sludge dewaterability. Volatile solids are typically reduced by 60–75% with final volatile matter contents of 40–50%.

*Author to whom correspondence should be addressed.
E-mail: lmohamed30@yahoo.com

Use of Effective Microorganisms (EM) is considered a global technique being used in more than 120 countries worldwide [6]. EM was originally developed as a microbial enhancer for soil applications and crop production in farming systems [7], but later was discovered to have very successful applications in the waste sector [8]

EM1 are the consortia of beneficial and naturally occurring microorganisms which are not chemically synthesized or genetically modified. The EM1 solution is the blending of effective microorganisms in molasses at low pH. EM1 has wide application in the field of agriculture, natural farming, livestock, gardening, composting, and bioremediation [9]. EM treated sludge is used as fertilizer as it is enriched with beneficial microorganisms [10].

EM is a mixture made up of groups of organisms that have a reviving action on humans, animals, and the natural environment [11]. It has also been described as a multi-culture of coexisting anaerobic and aerobic beneficial microorganisms [12]. Main species in EM include the following:

- Lactic acid bacteria—*Lactobacillus plantarum, L. casei, Streptoccus lactis*
- Photosynthetic bacteria—*Rhodopseudomonas palustrus, Rhodobacter spaeroides*
- Yeasts—*Saccharomyces cerevisiae, Candida utilis*
- Actinomycetes—*Streptomyces albus, S. griseus*
- Fermenting fungi—*Aspergillus oryzae, Mucor hiemalis* [13]

Activation of EM involves addition of 7 L of chlorine free water and 1.5 kg of brown sugar to 3 L of dormant EM one week prior to application. These ingredients were mixed together in either a 15 L or 20 L container and stored in an area with minimal temperature fluctuations. A major influence on the survival of microorganisms is temperature of their environment with significant temperature fluctuations impacting survival. The pH is also a determining factor. It was demonstrated that the pH of the EM should be approximately 4.5 [14].

This study examined the effect of co-digesting sewage sludge and agricultural residues (e.g., rice straw, grass clipping, sugar cane refuse, and maize stalks) in an anaerobic digester and found improvement in COD destruction, VSS destruction, and total alkalinity. The author arranged different residues according to improvement of effluent sludge characteristics as follows (1) rice straw, (2) grass clipping, (3) sugar cane refuse, and (4) maize stalks. Essential elements & heavy met-

als were observed in the effluent of the mixture of rice straw and sewage sludge to investigate it as fertilizer. Results indicated permissible concentration for agricultural use [14].

It was suggested that introducing EM1 into anaerobic treatment facilities helped to reduce unpleasant by-products of decomposition and also reduced production of residual sludge. These factors tend to suggest that theoretically EM1 should assist in treatment of wastewater by improving quality of water discharged and reducing volume of sewage sludge produced [15].

MATERIALS AND METHODS

The main objective here is to improve performance of treated thickened sludge by addition of rice straw as a source of organic carbon and EM1.

The sludge used in these experiments was thickened sludge, obtained from the gravity thickener of El-Berka wastewater treatment plant. Different ratios of rice straw and EM1 were mixed with thickened sludge to achieve a suitable mixing ratio to improve sludge treatment. A lab scale reactors were designed to achieve the objective of this study as an anaerobic conditions as shown in Figure 1.

Batch operation was divided into three stages. In these stages thickened sludge was mixed with different mixing ratios of EM1, and rice straw. The mixing ratio was as follows 0%, 10%, and 20% rice straw and 0, 1:250, 1:500, and 1:1000 EM1 for each run.

The batch operation with 20 days hydraulic retention time for each stage began on 01/06/2013 and finished on 02/08/2013. Physico–chemical analysis was carried out according to the American Standards Methods for examination of water and wastewater. Reactors performance was monitored by measuring total solids
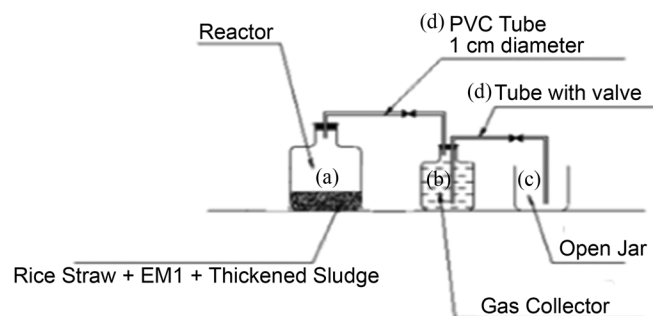

Figure 1. *Schematic diagram of reactor in lab scale. (a) 5L glass bottles with closed stoppers (Reactor), 3L working volume; (b) 3L glass bottles with closed stoppers filled with water to measure amount of gas released; (c) 3L glass bottles with closed stopper to measure displaced water; and (d) Bottles were connected with poly vinyl chloride (PVC) pipes.*

Table 1. Characteristics of Influent and Effluent Wastewater Sludge by Adding 0% Rice Straw and Different EM1 Concentrations for Retention Time 20 days.

Date	Samples	Temp. °C	pH	TS mg/l	TSS mg/l	VSS mg/l	COD mg/l	Alk mg/l	BOD$_5$ mg/l
1-6	Inlet Th. Sludge	27	6.9	28620	23500	14800	27204	1900	16200
20-6	outlet Th. sludge	28	7.2	49540	32900	11230	22260	3800	13356
1-6	Inlet Th. Sludge	27	6.9	28620	23500	14800	27204	1900	16200
20-6	1:1000 EM	30	7.3	52640	35670	6390	16330	4160	7398
1-6	Inlet Th. Sludge	27	6.9	28620	23500	14800	27204	1900	16200
20-6	1:500 EM	30	7.44	57190	32505	7460	14640	4600	8784
1-6	Inlet Th. Sludge	27	6.9	28620	23500	14800	27204	1900	16200
20-6	1:250 EM	31	7.5	62680	29500	9840	12380	4800	9828

(T.S.) and total volatile suspended solids (V.S.S.), pH, Chemical oxygen demand (COD), biological oxygen demand (BOD), alkalinity, and methane released.

RESULTS

Samples of influent were collected at the beginning of experiments. Effluent samples were collected after 20 days hydraulic detention time. Stage 1, chemical characteristics of influent and effluent thickened sludge were measured and are displayed in Table 1 by adding 0% rice straw with 0%, 1:250, 1:500, and 1:1000 EM1 to thickned sludge. Figure 2 shows COD and total VSS for sewage sludge at 0% rice straw and different ratios of EM1 additions.

Stage 2, Chemical characteristics of influent and effluent thickened sludge were measured and are displayed in Table 2 with adding 10% rice straw with 0%, 1:250, 1:500, and 1:1000 EM1 additions. Figure 3 shows COD and total VSS for sewage sludge at 0% rice straw and for different ratios of EM1 additions.

Stage 3, Chemical characteristics of influent and effluent thickened sludge were measured as shown in Table 3 with addition of 20% rice straw and 0%, 1:250, 1:500, and 1:1000 EM1 additions. Figure 4 shows COD and total VSS for sewage sludge at 20% rice straw and for different ratios of EM1.

Measuring Methane

Methane is one of the major products in digester operation. Quality of biogas depends on relative amounts of CH_4 and CO_2 ultimately produced. Gases released from pilot reactors were difficult to measure because they escape with water. Therefore, biogas production was determined by means of a material balance. This may be done by measuring COD of all streams including biogas which enter and exit the reactor. For the product of the gas phase carbon dioxide has zero COD since it is fully oxidized. The COD of methane may be calculated from its oxidation reaction.

$$CH_4 + 2O_2 \rightarrow CO_2 + H_2O$$

Figure 2. *(a) Inlet and Outlet COD values of TH.S with adding 0% R.ST and different EM1 concentrations (stage 1) and (b) Inlet and Outlet Total VSS values of TH.S with adding 0% R.ST and different EM1 concentrations (stage 1).*

Table 2. Characteristics of Influent and Effluent Wastewater Sludge with Addition of 10% Rice Straw and with Different EM1 Concentrations.

Date	Samples	Temp. ºC	pH	TS mg/l	TSS mg/l	VSS mg/l	COD mg/l	Alk mg/l	BOD$_5$ mg/l
23-6	Inlet Th. Sludge	28	6.9	28620	23500	14800	27204	1900	16200
12-7	Outlet Th. sludge	30	7.54	49450	32900	11230	22260	3800	13360
23-6	Inlet Raw Sludge	28	6.9	28620	23500	14800	27204	1900	16200
12-7	0% EM	31	7.3	59390	40650	7450	13170	3950	7900
23-6	Inlet Th. Sludge	28	6.9	28620	23500	14800	27204	1900	16200
12-7	1:1000 EM	32	7.6	62640	38900	5250	14340	4800	8700
23-6	Inlet Th. Sludge	28	6.9	28620	23500	14800	27204	1900	16200
12-7	1:500 EM	31	7.1	69730	36400	4970	13320	5100	8000
23-6	Inlet Th. Sludge	28	6.9	28620	23500	14800	27204	1900	16200
12-7	1:250 EM	33	6.8	74360	35500	4520	11270	5400	6700

DISCUSSION AND CONCLUSIONS

It was noticeable that addition of EM1 to thickened sewage sludge reduced offensive odours of sludge. Next, it was shown that rice straw and EM1 keeps the pH value near to the normal conditions. The characteristics of EM1 and rice staw increase pH values due alkalinity of EM1 and the organic nitrogen in rice straw that would be converted into ammonia during the digestion process. Therefore, the addition of rice straw to the EM1 balanced pH values.

One of the main objectives of anaerobic digestion is decomposition and reduction of the organic fraction of feed sludge and in sludge analysis the organic fraction is estimated by determining volatile content of sludge. Therefore, it was found that by increasing the ratio of rice straw and EM1the total solids increased and VSS decreased because after digestion sludge volume was reduced due to separation of free water and sludge sta-

bilized into digested sludge and gases. Also, solid concentration increased by co-digested sludge rice straw and EM1. The effluent concentration increased and helped in sludge dewaterability. Creation of antioxidant environments by EM assists in enhancement of solid-liquid separation the foundation for cleaning water.

It was shown in three stages that addition of EM1 to thickened sewage sludge decreased effluent COD values and concentration ratio of EM1 was increased the amount of microorganisms organic matter in the reactor increased so COD value decreased. This is because COD corresponds to amount of oxygen required to oxidize the organic fraction. More oxygen is consumed. BOD ratios also decrease by increasing concentration of rice straw and EM1. COD reduction reaches 70% at EM1 1:250 and rice straw reaches 20% and total VSS reduction reaches 74% at EM1 1:250 and rice straw 20%.

Aerobic co-digesting of thickened sludge with rice straw and EM1 improved the digestion process. The
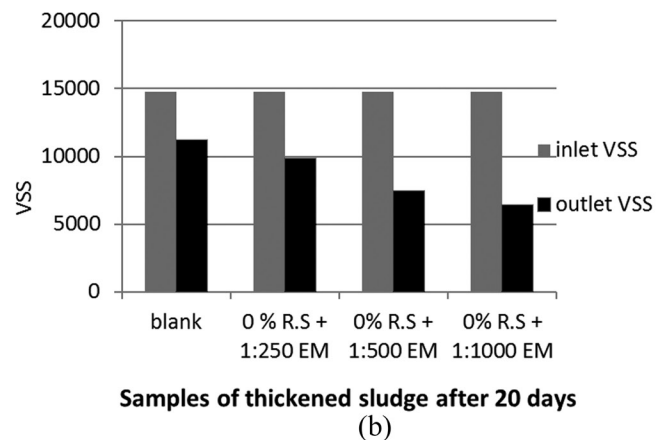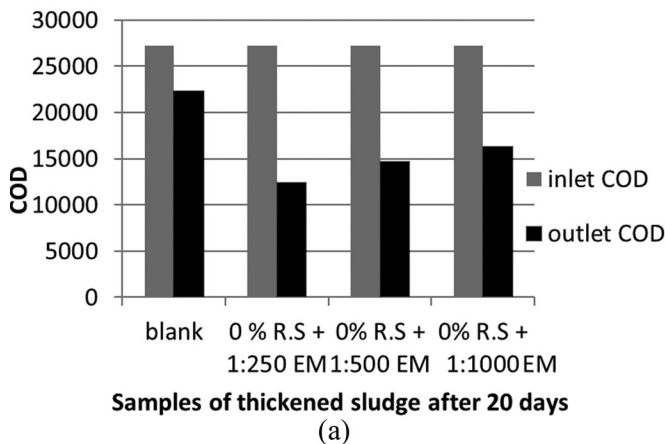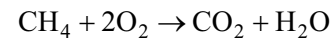

Figure 3. *(a) Inlet and Outlet COD values of TH.S with adding 10% R.ST and different EM1 concentrations (stage 2) and (b) Inlet and Outlet Total VSS values of TH.S with adding 10% R.ST and different EM1 concentrations (stage 2).*

Table 3. Characteristics of Influent and Effluent Wastewater Sludge with Addition of 20% Rice Straw and for Different EM1 Concentrations.

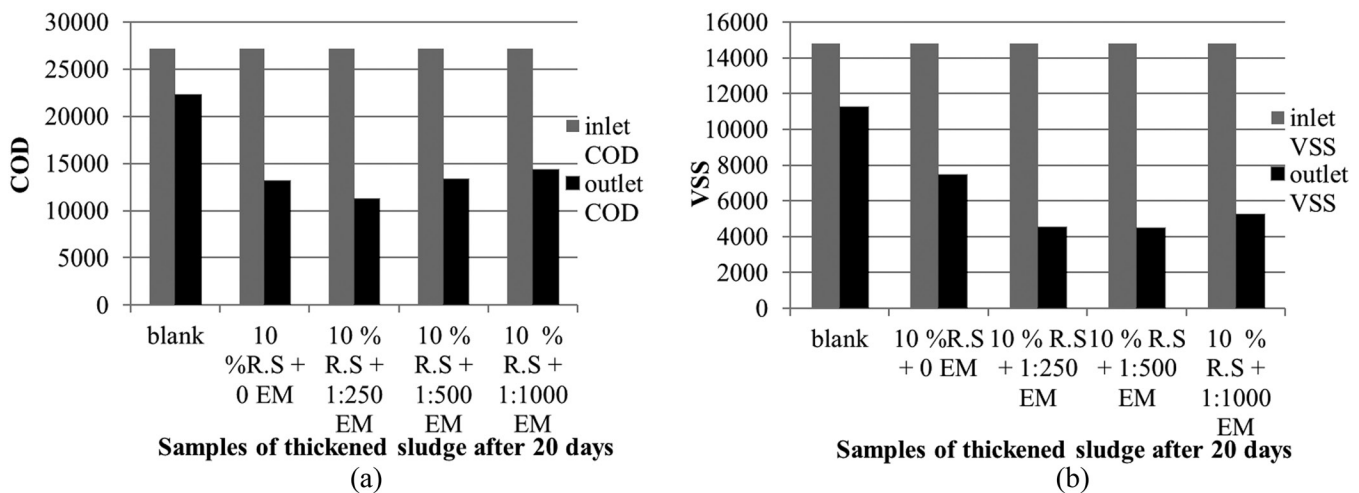| Date	Samples	Temp. ºC	pH	TS mg/l	TSS mg/l	VSS mg/l	COD mg/l	Alk mg/l
14-7	Inlet Th. Sludge	30	6.9	28620	23500	14800	27204	16800
2-8	Outlet Th. sludge	32	7.2	49540	32900	11230	22260	13360
14-7	Inlet Th. Sludge	30	6.9	28620	23500	14800	27204	16800
2-8	0% EM	31	7.4	76460	42700	6350	12560	7500
14-7	Inlet Th. Sludge	30	6.9	28620	23500	14800	27204	16800
2-8	1:1000 EM	33	7.74	79530	42850	4380	9910	5950
14-7	Inlet Th. Sludge	30	6.9	28620	23500	14800	27204	16800
2-8	1:500 EM	33	7.6	82560	40200	4270	9530	5700
14-7	Inlet Th. Sludge	30	6.9	28620	23500	14800	27204	16800
2-8	1:250 EM	34	7.53	88450	37400	3850	8340	5000
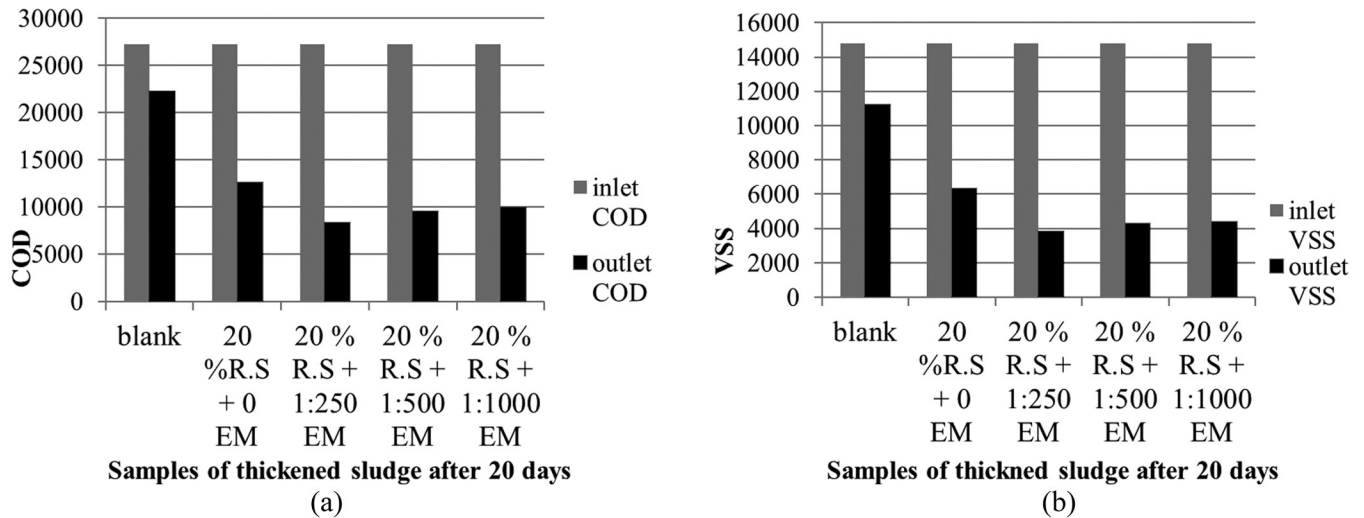
Figure 4. *(a) Inlet and Outlet COD values of TH.S with adding 20% R.ST and different EM1 concentrations (stage 3) and (b) Inlet and Outlet Total VSS values of TH.S with adding 20% R.ST and different EM1 concentrations (stage 3).*
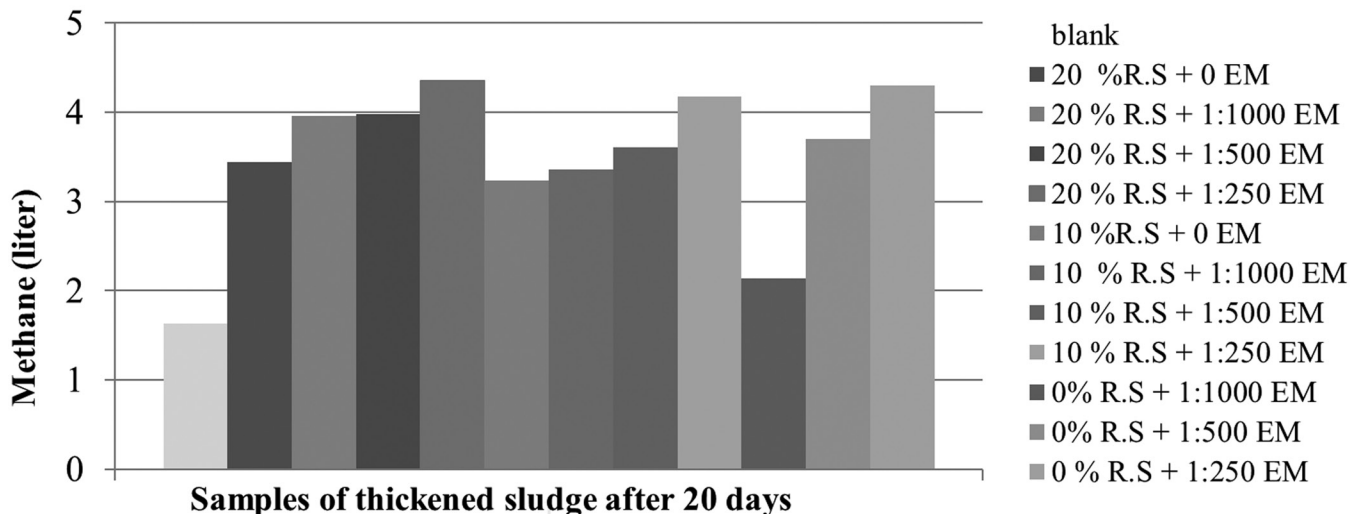

Figure 5. *Methane values for thickened sludge and different ratios of EM1.*

most suitable ratio of rice straw and EM1 to be added to thickened sewage sludge according to the COD removal is 1:250 EM1 and 20% rice straw (w/w). Mixing rice straw and EM1 with thickened sludge increases efficiency of the anaerobic digestion process. EM1 reduced pH to near normal conditions. Therefore, application of such sludge to crops would not produce alkali conditions.

REFRENCES

1. Metcalf & Eddy, (2003). ''Wastewater engineering treatment and re-use''. Fourth edition, USA.

2. Veeken, A.H.M., Hamelers, H.V.M., 1999. Removal of heavy metals from sewage sludge by extraction with organic acids. *Water Science and Technology 40*, 129–136.

3. Elliott, H.A. (1986) 'Land Application of Municipal Sewage Sludge', in *Journal of Soil and Water Conservation*, (41) pp 5–10.

4. Dr. Seham M. H. Hendy" Regional "Wastewater Management and Reuse in Egypt" Workshop on Health Aspects of Wastewater Reuse in Agriculture, Amman, Jordan 30 October–3 November 2006.

5. Marcos von Sperling, Carlos A. Chernicharo, (2005). "Biological wastewater treatment in warm climate regions". IWA Publishing, USA.

6. EM America Website 2009. http://www.emamerica.com/home/effective-microorganisms

7. Higa, T; Parr, J.F. 1994. Beneficial and Effective Microorganisms for a Sustainable Agriculture and Environment. International Nature Farming research Center, Japan.

8. Okuda A., Higa, T. 1995. Purification of Waste Water with Effective Microorganisms and its Utilization in Agriculture. University of the Ryukyus, Okinawa, Japan. http://www.emrojapan.com/db/0b792684a1a6037b0b7159c95310e046.pdf

9. Daly Mj, Arnst B (2005) The Use of an Innovative Microbial Tecnology (EM) for Enhancing Vineyard Production and Recycling Waste from the Winery Back to the Land, the 15th IFOAM Organic World Congress Adelaide.

10. Miyajima M, Nagano N, Higa T (1995) suppression of dioxin generation in the garbage incinerator, using EM (effective microorganisms) , EM-Z,AND EM-Z ceramics powder, college of agriculture, university of Ryukus.

11. Higa, T. 1995, 'What is EM Technology', College of Agriculture, University of Ryukyus, Okinawa, Japan.

12. Freitag, D.G. 2000 (updated 3 May 2000, accessed 27 Aug 2002), 'The use of Effective Microorganisms (EM) in Organic Waste Management' *Effective Microorganisms @ emtrading.com*, http://emtrading.com/em/htmlpapers/emwasterepfreitag.html

13. Diver, S. 2001 (updated 11 Oct 2001, accessed 27 Aug 2002), 'Nature Farming and Effective Microorganisms', *Rhizosphere II: Publications, Resource Lists and Web Links from Steve Diver*, http://ncatark.uark.edu/~steved/Nature-Farm-EM.html

14. Ezzat A.H., M.R. Ehab and M.F. Ayman, 2007. Enhancing the efficiency of anaerobic sludge digester by mixing sewage sludge with agriculture residues" Ain Shams University international conference on environmental engineering, 1: 313–326.

Fine-Scale Prediction of Roadside CO and NOx Concentration Based on a Random Forest Model

BINGYUE SONG*, JIANPING WU, YANG ZHOU and KEZHEN HU

Department of Civil Engineering, Tsinghua University, Room 310, Old Hudraulic Building, Tsinghua University, Beijing, China, 100084

ABSTRACT: In urban areas, motor vehicle emissions have been identified as the major source of urban air pollution, for they disperse and gather near roadside microenvironments are influencing travelers' health. In this paper, Random Forest was employed to build a-fine scale predicting model of roadside pollutant concentration, using traffic, meteorological and local geographic factors measured by a mobile monitoring platform in four urban roads with high spatial and temporal sampling interval. Models were built based on 700 5-min observations with MSE of CO prediction model being 8.3 and that of NOx model being 8.9. OOB examination assured its generalization ability and indicated that the models were converged with the tree number increased up to approximate 300 for CO model and 450 for NOx model, respectively. Models were validated by the other 125 5-min observations with desirable prediction results, which showed better prediction performance than ANN model.

In urban area, traffic-related pollutants contribute a significant proportion to roadside microenvironment, which needs to be characterized since people spend a substantial percent of their outdoor time in this environment. Exposure to CO is associated with an increase in mortality from cardiovascular disease; exposure to NOx is directly associated with adverse effects on asthma disease [1] and respiratory system [2].

LITERATURE REVIEW

IN general, traffic-related emissions were primary exhaust from on-road vehicles, influenced by vehicle turbulence and local meteorological conditions, and dispersed among roadside microenvironment. Extensive research has been conducted on the joint application of emission model and dispersion model to characterize the roadside air quality. For instance, COPERT and OSPM [3] and adjusted MOVES+AERMOD [4]. However, the emission models could not accurately stand for the real time on-road emission character [5]. Besides, Limitations in dispersion model [6–8] restricted the application of such models in predicting roadside pollutant concentration. Researchers conducted field experiment in specific locations [8,9] with measured variables including wind speeds, wind direction, traffic volume, occupancy, vehicle speed and headway as the input of ANN (Artificial Neural Networks) model to predict CO or NOx concentration, with the desirable prediction accuracy.

Initially, ANN have been achieved desirable performance in predicting CO or NOx concentration in different temporal and spatial resolution [8,9]. However, ANN could not indicate the relationship between traffic and roadside concentrations. Thus, multi-regression method was utilized to examine such relationships [10], to optimize the regression model, a generalized additive model was introduced. However, collinearity in multiple regression models and concurvity in generalized additive model might cause a discrepancy of quantitative relationship between traffic variables and the predicted concentration, influencing the prediction ability of the proposed model.

Random Forest (RF) was proposed by Breiman in 2001 [12], which creates multiple classification and regression (CART) trees, can properly solves the problems of collinearity and concurvity existing in regression analysis and generalized additive model. In addition, RF also can provide a determinate relationship between the traffic and roadside concentration without losing prediction accuracy [13,14].

EXPERIMENTAL

Study Areas and Monitoring Protocol

Taking road characteristics, traffic density and roadside building into account, four roads (Figure 1) were

*Author to whom correspondence should be addressed.
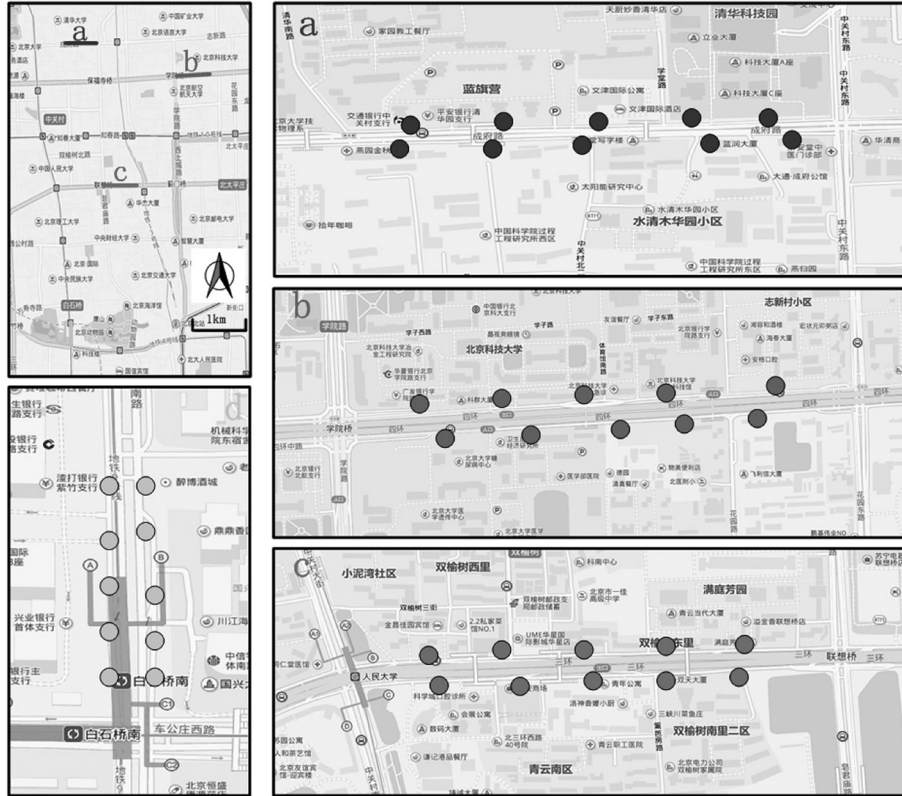E-mail: songbingyue@gmail.com

Figure 1. *Four study areas and sampling points.*

selected in this study, two urban expressways (b,c), one arterial road (d) and one bypass (a). Mobile monitoring platform can sample multi-source data simultaneously by instrumented transport equipment, meteorological and environmental instruments [14–17]. In this study, the vehicle monitoring platform was based on an IVECO turbo vehicle with CO (Model 48i-TLE, Thermo Scientific, USA), NOx (Model 42i, Thermo Scientific, USA) measuring device, and the sampling inlets were approximately 3.2m above ground level. The temporal resolution was 10s with an output resolution of 1min. GPS/INS RT2500 is used to represent the average speed of the fleet. In addition, the surveyor used a Sony camera (HDR-XR160E, Sony Corporation) with high time resolution to concurrently record traffic condition and traffic volume.

Ten sampling locations were arranged for each road with 5 in each direction, and temporal resolution was approximate 100m along road direction. In each direction, 5 sampling locations were approximately evenly distributed along road direction. For each road, we took a 5-min stop at each sampling point, while local traffic volume, instantaneous speed, number of truck and meteorological parameters were recorded per minute in the meantime. A loop (10 location × 5 min) measure-

ment of one road will cost approximate 60 minute to complete. In general, we took 4 loop measurements in one day, two for peak time and two for off-peak time. Monitoring campaign was completed during weekday from March to June, 2014 in Beijing, China.

In this study, the selection of traffic variables is partially referred to research [18]: real-time traffic and diesel truck count, and average speed, as well as meteorological characteristics. Those variables were typical and direct indicators of traffic pattern, and are easy to obtain by the public.

METHDOLOGY

In this paper, methodology was based on Random Forest to make regression analysis in fine scale over street level, with the predictor vector considered as the predictor variable and pollutant concentration as the prediction result.

A Random Forest is a classifier consisting of a collection of tree-structured classifiers $\{h(x,\Theta_k), k = 1, . . .\}$, where the $\{\Theta_k\}$ are independent identically distributed random vectors and each tree casts a unit vote for the most popular class at input [11]. Random forests for regression are formed by growing trees depend-

ing on a random vector Θ such that the tree predictor $h(X,\Theta)$ takes on numerical values as opposed to class labels [11].

In this article, RF algorithm was programmed in Matlab2012R platform, training data was firstly ob-

tained from source data set by bagging method [19]. Then, every tree starts with a "root node" that contains the training data from which the tree will be grown. The training data are then partitioned into two "child nodes" based on the value of an independent predictor
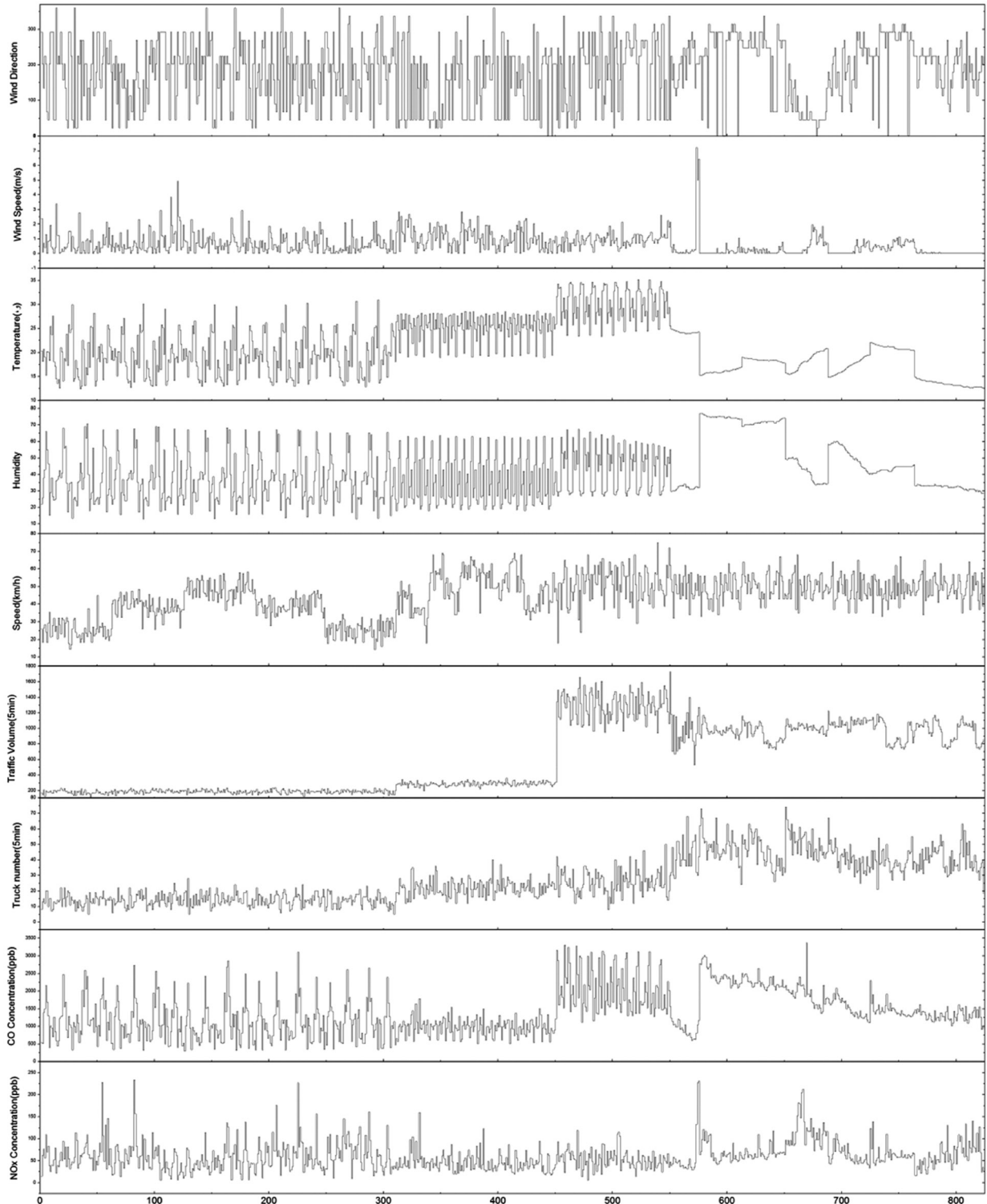

Figure 2. *Description of data in 5-min scale.*

factor. The resulting child nodes each contains a subset of the training data. Each child node may be further partitioned, again based on the value of an independent predictor factor. This process continues until a set of partitioning criteria are no longer met, resulting in terminal nodes. Terminal nodes, by definition, cannot have offspring. The collection of terminal nodes forms a complete partition of the observations in the root node.

There are two reasons for using bagging method. The first is that the use of bagging seems to enhance accuracy when random features are used [11]. The second is that bagging can be used to give ongoing estimates of the generalization error of the combined ensemble of trees, as well as estimates for the strength and correlation. In this paper, Forest-RI was employed to take the feature selection. For input data, source data were scaled into the range of [–1, 1] in order to keep the data in same scale for analysis. Taking into account of computation time of RF, the maximum tree number in this paper was 1000.

RESULTS AND DISCUSSION

Overview of Sampling Results

After 40 sampling days, we obtain approximate 4870 min observations of pollutant concentration as well as the predictor variables. Road a, Road b, Road c and Road d accounted for 35.6%, 19.3%, 29.1% and 16% of the data, respectively. Since traffic volume is a quite volatile parameter, higher resolution of temporal data might increase the randomness. To reduce sampling randomness and select time interval during which variables were rather stable, 5-min was seen as the unit, And traffic volume was aggregated while the other observations were averaged. After such process,

824 5-min observations were obtained and considered as the training data. Summary of such data were illustrated in Figure 2.

Correlations Among Predictor Variables

Firstly, 5-min sets of data were conducted correlation analysis to understand the relationship among them. For relationship between pollutants and predictors, results indicated in Table 1 showed that CO concentration is significant correlated with humidity and volume, while NOx has a weak relationship with humidity and aspect ratio. Besides pollutant concentrations, it can be seen that volume has positive correlation with that of truck number during sample intervals. In addition, correlation shown between speed and volume was 0.44, indicating that using neither variable alone could well represent the traffic state. In sum, for predictive variables, most have a moderate relationship with each other, which has limited the application of regression method, since the collinearity among them would decrease the prediction accuracy in the model.

Prediction Result of Random Forest

704 5-min observations were used as training data, and the left 120 5-min observations as testing data. Testing data contains 30 5-min observations of each road. In training the model, OOB (out of bag) was employed in order to validate the generalization of the training model, like cross-validation method, ensuring the complete independence of training data and testing data. OOB also enhanced the model prediction accuracy and the convergence of the model by controlling two random variables: split feature and total number of trees. Figure 3 demonstrated that model converged

Table 1. Correlation Coefficient between Predictive Variables and Pollutant Concentration.

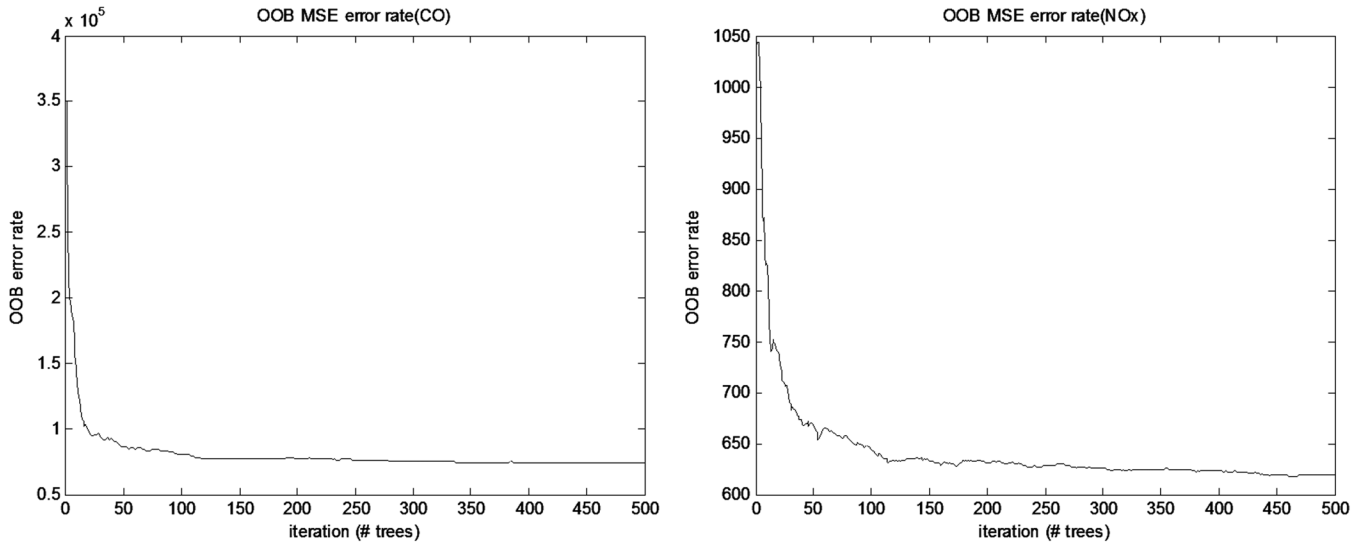|	CO	NOx	Wd	Ws	Temp	Humi	Aspe	Speed	Vol	Hea
CO	1									
NOx	0.47	1								
Wd	−0.02	−0.24	1							
Ws	−0.24	−0.15	−0.008	1						
Temp	0.0009	−0.25	−0.03	0.37	1					
Humi	0.65	0.27	0.1	−0.3	−0.29	1				
Aspe	0.2	0.28	0.04	−0.22	−0.47	0.18	1			
Speed	0.18	−0.08	−0.01	0.03	0.16	0.14	−0.22	1		
Vol	0.57	0.13	0.10	−0.14	0.16	0.30	0.14	0.44	1	
Hea	0.44	0.22	0.07	−0.29	−0.2	0.36	0.31	0.39	0.69	1

Figure 3. *Relationship between tree numbers in RF and OOB error rate.*

when the tree number of RF increased approximate to 300 and 450 for CO model and NOx model, respectively.

In training the model, important predictors can also be identified by RF. In Figure 4, results illustrated that important predictors were humidity, traffic volume and temperature in CO prediction model, while in NOx prediction model, rather important predictors were aspect ratio, humidity and temperature. The results demonstrated that roadside pollutant concentration was related to various meteorological conditions as well as local geographical characteristics, and prediction merely by traffic predictors might contribute to significant variance of accuracy.

MSE (mean squared error) was employed to assess the model, with the results of 8.3 (scaled data into [−1,1]) in CO concentration RF regression tree and 5.9 (scaled data into [−1,1]) in NOx concentration RF regression tree, indicating that the models were pretty well constructed to fit the training data according to the RF theory.

When the model was applied in predicting CO and NOx concentration, ANN model was also built for comparison. ANN was constructed in traditional three-layer layout with same input variable number as RF, with 6 hidden layers and RBF (Radical Basis Function) active function. The model output was the corresponding pollutant concentration and the process was imple-
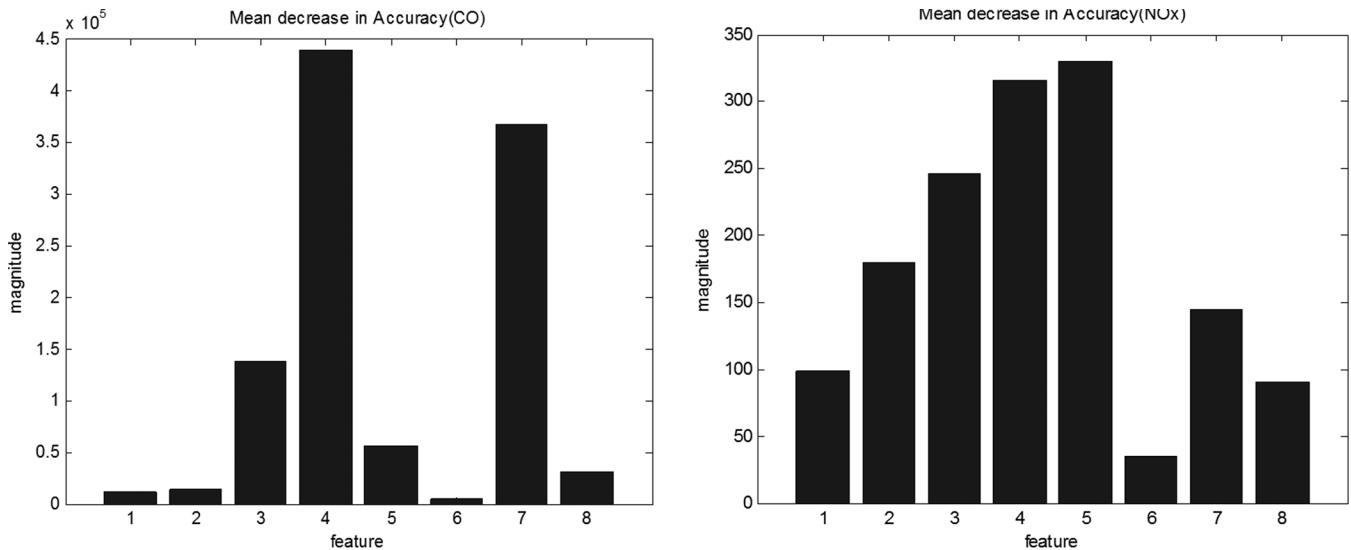

Figure 4. *Important predictors in training model (feature 1~8 represent wind direction, wind speed, temperature, humidity, aspect ratio, speed, volume and truck number, respectively).*
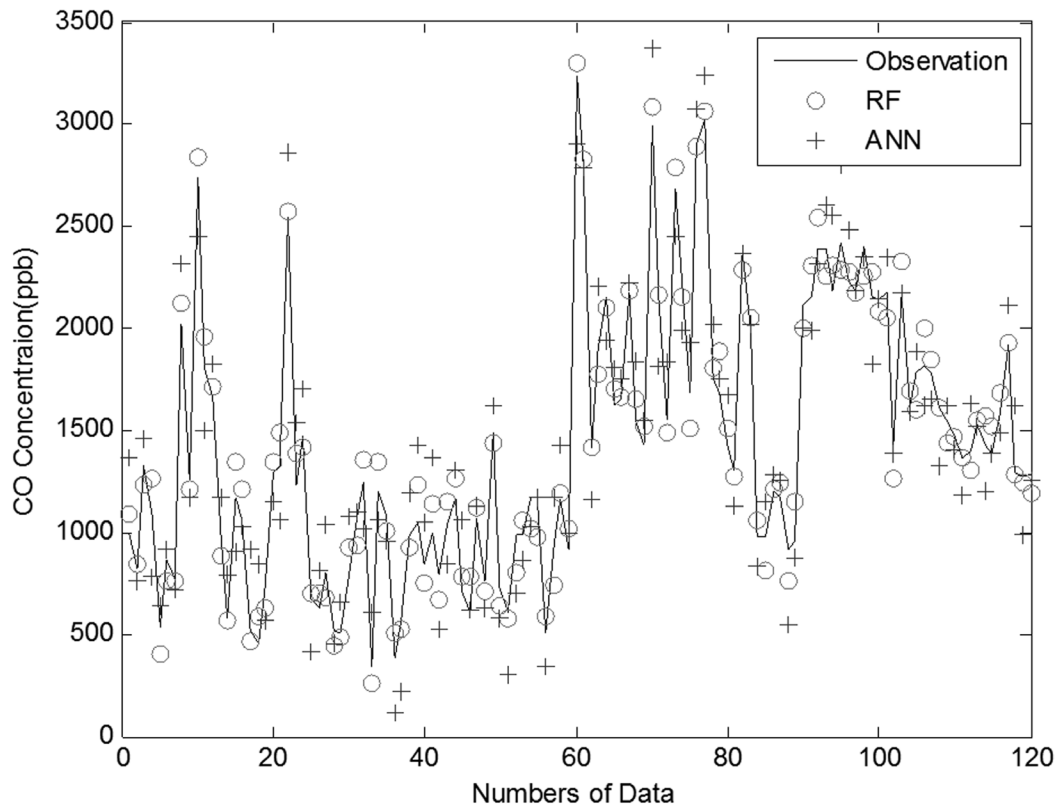
Figure 5. *Comparison of Results Predicted by RF model and ANN model (test data number=120).*

mented in the platform of Matlab 2012R. 120 5-min observations were considered as testing data, and the prediction results were demonstrated in Figure 5. It is obvious that RF shows better prediction ability than that of ANN, both in CO and NOx prediction performance. MSEs in prediction process were 57.15 and 43.60 for CO and NOx, respectively, which is in accordance with that shown in Figure 5. Therefore, the prediction model based on RF can be applied in predicting CO and NOx concentration in roadside microenvironment, which implies that RF model can be a potential model in implementing prediction with higher prediction accuracy.

CONCLUSIONS

In this study, RF theory was utilized in a fine-scale prediction of CO and NOx concentrations in roadside microenvironment with desirable results using traffic, meteorological and local geographic factors, which implied that if such factors were available, roadside traffic-related pollutant concentrations can be modelled in a fine scale. In that case, mapping traffic-related pollutant concentration in street level over ground level can become possible, which will help

to understand and characterize variation of roadside pollutant concentration in high spatial and temporal resolution. Evidently, such a fine-scale air pollution prediction would facilitate the development of urban epidemiological study.

ACKNOWLEDGEMENTS

REFERENCES

1. Delfino, R.J., Gong Jr., H., Linn, W.S., Hu, Y., Pellizzari, E.D. Asthma symptoms in Hispanic children and daily ambient exposures to toxic and criteria air pollutants. *Environ. Health Perspect.s*, Vol. 111, No. 4, 2003, pp. 647–656.

2. Maitre, A., Bonneterre, V., Huillard, L., Sabaties, P., Gauemaris, R.D. Impact of urban atmospheric pollution on coronary disease. *Eur Heart J.*, Vol. 27, No. 19, 2006, pp. 2275–2284.

3. Giannouli, M., Kalognomou, E.A., Mellios, G., *et al.* Impact of Euro-

pean emission control strategies on urban and local air quality. *Atmos. Environ.*, Vol. 45, No. 27, 2011, pp. 4573–4762.

4. Liu, H.B., Chen, X.H., Wang, Y.Q., *et al.* Vehicle Emission and Near-Road Air Quality Modeling for Shanghai, China. In *Transportation Research Record: Journal of the Transportation Research Board*, No. 2340, Transportation Research Board of the National Academies, Washington, D.C., 2013, pp. 38–48.

5. Fujita, E. M., Campbell, D. E., Zielinska, B., *et al.* Comparison of the MOVES2010a, MOBILE6.2, and EMFAC2007 mobile source emission models with on-road traffic tunnel and remote sensing measurements. *J. Air Waste Manage. Assoc.*, Vol. 62, No. 10, 2012, pp. 1134–1149.

6. Harrison, R. M., Jones, A. M. and Barrowcliffe, R. Field study of the influence of meteorological factors and traffic volumes upon suspended particle mass at urban roadside sites of differing geometries. *Atmos. Environ.*, Vol. 38, No. 37, 2004, pp. 6361–6369.

7. Blocken, B., Stathopoulos, T., Carmeliet, J. and Hensen, J. L. Application of computational fluid dynamics in building performance simulation for the outdoor environment: an overview. *J. Build Perform Simu.*, Vol. 4, No.2, 2011, pp. 157–184.

8. Moseholm, L., Silva, J. and Larson, T. Forecasting carbon monoxide concentrations near a sheltered intersection using video traffic surveillance and neural networks. *Transport Res D-TR E*, Vol. 1, No.1, 1996, pp. 15–28.

9. Cai, M., Yin, Y. and Xie, M. Prediction of hourly air pollutant concentrations near urban arterials using artificial neural network approach. *Transport Res D-TR E*, Vol.14, No.1, 2006, pp. 32–41.

10. Fruin, S., Westerdahl, D., Sax, T. *et al.* Measurements and predictors of on-road ultrafine particle concentrations and associated pollutants in Los Angeles, *Atmos. Environ.*, Vol. 42, No. 2, 2008, pp. 207–219.

11. Breiman, L. Random forests. *Machine Learning,* Vol. 45, No.1, 2001, pp. 5–32.

12. Deng, C., Guo, M.Z. A new co-training-style random forest for computer aided diagnosis. *J. Intell Inf Syst.*, Vol. 36, No. 3, 2011, pp. 253–281.

13. Wu, J., Jiang, C.S. Houston, D. Automated time activity classification based on global positioning system (GPS) tracking data. *Environ. Health*, Vol. 10, No. 101, 2011.

14. Hagler, G.S.W., Thoma, E.D., Baldauf, R.W. High-resolution mobile monitoring of carbon monoxide and ultrafine particle concentrations in a near-road environment. *J. Air Waste Manage. Assoc.*, Vol. 60, No.3, 2010, pp. 328–336.

15. Choi, W., He, M., Barbesant, V., Kozawa, K.H., Mara, S., Winer, A.M., Paulson, S.E. Prevalence of wide area impacts downwind freeways under pre-sunrise stable atmospheric conditions. *Atmos. Environ.,* Vol. 62, 2012, pp. 318–327.

16. Hu, S., Paulson, S.E., Kozawa, K., Mara, S., Fruin, S., Winer, A.M. Observation of elevated air pollutant concentrations in a residential neighborhood of Los Angeles California using a mobile platform. *Atmos. Environ.*, Vol. 51, 2012, pp. 311–319.

17. Baldauf, R.W., Heist, D., Isakov, V., Perry S, *et al.* Air quality variability near a highway in a complex urban environment. *Atmos. Environ.*, Vol.64, 2013, pp. 169–178.

18. Li, L.F., Wu, J., Hudda, N. Modeling the Concentrations of On-Road Air Pollutants in Southern California. *Environ. Sci. Technol.*, Vol. 47, No. 16, 2013, pp. 9291–9299.

19. Breiman, L. Bagging predictors. *Machine Learning*, Vol. 26, No. 2, 1996, pp.123–140.

Strength and Leaching Characteristics of Heavy Metal Contaminated Soils Solidified by Cement

YU-YOU YANG[1,*], HAO-LIANG WU[2,*] and YAN-JUN DU[2]

[1]School of Engineering and Technology, China University of Geosciences (Beijing), Beijing 100083, China
[2]Institute of Geotechnical Engineering, School of Transportation, Southeast University, Nanjing 210096, China

ABSTRACT: Portland cement was used to stabilize Zn and Pb contaminated soils sampled from a mining area. A series of tests including unconfined compression test, pH test, toxicity characteristic leaching procedure (TCLP), and synthetic precipitation leaching procedure (SPLP) were conducted in order to investigate the effects of curing time and cement content on the unconfined compressive strength and leachability of lead and zinc. The test results show that at the curing time of 28 d, the dry density and UCS of soil with 8% cement are approximately 2% higher than and 1.6 times, respectively, those of the soil with 4% cement. The pH values of TCLP and SPLP leachate drop by 1.19 to 1.23 and 0.34 to 0.38, respectively when the curing time increases from 0 to 28 d. Moreover, the test results also show that the concentrations of leached Pb and Zn decrease with increasing curing time.

LITERATURE REVIEW

THE abundant mineral resources in China are a major source of energy and industrial raw materials. However, the excessive exploitation of mineral resources has exposed serious impacts to surrounding environment. Soil contamination by heavy metals in the mining areas primarily results from down-hole mineral processing in metal mines, effluent discharge, tailings and abandoned mines [1]. Due to long-term water scouring and natural sedimentation, there exists a widespread and severe soil contamination in mining areas, resulting in potential geoenvironmental risks [2]. Heavy metal contaminated soils can cause deterioration in the local biosphere and expose environmental threats to eco-system [1]. It is reported that the concentrations of Pb and Zn in the soils of Hunan Huangshaping Lead-Zinc Mining Area are 21 times and 29 times, respectively, higher than their background values [3]. Therefore, treatment of heavy metal contaminated soils in mining areas is of great importance.

The commonly used technologies of treating heavy metal contaminated soils include natural attenuation, isolation, and remediation [4–5]. Previous studies have investigated the use of phytoremediation and bioremediation methods for remediating organic-contaminated

industrial soils and farmland in China. Limited studies have been done on electrokinetic remediation for heavy metal contaminated soils [6]. Nevertheless, remediation of contaminated soils in the mining areas receives limited attention; the electrokinetic remediation for lead (Pb) contaminated soils has high cost and needs relatively long time [7].

Solidification/stabilization (S/S) is used widely in treating heavy metal contaminated soils. The prevailing binders for S/S are Portland cement and cement-based cementitious materials. Solidification/stabilization by cement materials involves mechanical mixing of cement and contaminated soils and immobilizing the heavy metals by encapsulation, sorption and precipitation (e.g., metal hydroxides). As a result, diffusive properties of heavy metals will be lowered down and consequently satisfy environmental standards [8–9]. Minocha *et al.* [10] conducted a study on the early strength characteristics of Cu-contaminated slurry solidified by Portland cement. However, Lee [11] indicated that the strength of the cement-solidified contaminated soils decreased with increasing Pb concentration. Stepanova *et al.* [12] found that chlorides of Mn, Co, Ni, Cu, Zn and other heavy metals could react with the silicates and aluminates in cement, generating compounds that hinder its strength development. The toxicity characteristic leaching procedure (TCLP) test and synthetic precipitation leaching procedure (SPLP) test are widely used in many countries to study the

*Authors to whom correspondence should be addressed.
E-mail: yangyuyou@cugb.edu.cn; wuhaoliang90@163.com

leaching characteristics of pollutants in least favorable conditions in order to assess the safety of solidified contaminated soils.

In this study, a series of laboratory tests were conducted on cement solidified heavy metal contaminated soils sampled from a mining area, including unconfined compressive strength (UCS) test, toxicity characteristic leaching procedure (TCLP) test, and synthetic precipitation leaching procedure (SPLP) test. The effects of curing time and cement content on the moisture content, dry density, q_u, concentration of leached Pb and Zn are discussed. An empirical equation is proposed for quantifying relationship between $q_{u,t}$ and leached concentration of Zn for the solidified soils.

MATERIALS AND METHODOLOGY

Materials

Contaminated soils used in this study are sampled from the subsurface of a tailings pond of a nonferrous metal mine in the Hunan Province. The soils were sampled from the typical site at a depth of 0 to 0.5 m below the ground surface. The main physical and chemical parameters of the samples are shown in Table 1. The Atterberg limits were tested as per ASTM D4318 (ASTM 2010). Based on the Unified Soil Classification System, the soil is classified as low-plasticity clay (CL). The soil pH was tested as per ASTM D4972 (ASTM 2001). Heavy metal concentration was measured using a "quadri-acid digestion method" (GB/T 17141-1997). The results show that the sampled soil is primarily contaminated by Pb and Zn. Test results show that the concentrations of Pb and Zn in the soils are in the range of 4230–7550 mg/kg and 3200–5600 mg/kg, respectively. For simplification, this study only considers the contamination of Pb and Zn in the soil.

Cement used in the tests is #32.5 Portland cement produced in Nanjing, and its chemical constituents, determined by X-ray florescence spectrometry analysis, are shown in Table 2.

Sample Preparation

Prior to the sample preparation, all the soils sampled from the typical sites were mixed evenly. The

Table 1. Major Physical and Chemical Properties of the Soil.

Property	Value
Natural water content, w_n (%)	28.3
Specific gravity, G_s	2.75
Plastic limit, w_P (%)	22.6
Liquid limit, w_L (%)	43.5
Soil pH	7.93

mixed soil was air-dried, smashed and sieved through a 1 mm sieve. Predetermined volume of distilled water was added into soil until the water content reached approximately 22%; then the soils were mixed using an electronic mixer. Samples were made in cylindrical PVC pipe molds with an inner diameter of 50 mm and a height of 100 mm. Vaseline was uniformly applied to the inner wall of molds prior to the soil filling in the mold. Each soil sample had the same mass, and the filling was conducted in five stages. After each stage of filling, the sample was shaken manually for 2 min to remove entrapped air bubbles. When the final filling was completed, the top and bottom of the sample were covered with a PVC lid. The samples were then cured at a temperature at $20 \pm 3°$ and relative humidity of 95%. After curing for 1 to 3 d depending on the cement content, the samples were carefully extruded from the molds using hydraulic jack, weighed, wrapped by vinyl films, and cured again under the standard condition until the designated time. The curing time selected in this study included 3, 7, 14 and 28 d. Two cement contents were set, i.e., 4% and 8% (dry weight soil basis). Hereinafter through the entire text, figures and tables, a denotation of $C_{i\text{-}j}d$ represents a sample with cement content of i% and a curing time of jd. Triplicates were prepared with a given cement content and curing time.

Test Methods

For each sample prior to the unconfined compression test (UCT), its bulk density was measured. The UCT was performed as per Test Methods of Soils for Highway Engineering JTG E40-2007. The strain rate was controlled as 1%/min based on ASTM D2166 (ASTM 2006). After the UCT, certain mass of soil was sampled from the broken samples and was tested for its

Table 2. Chemical Oxide of the Cement Tested.

Oxide	CaO	SiO$_2$	Al$_2$O$_3$	SO$_3$	Fe$_2$O$_3$	MgO	MnO	K$_2$O	TiO$_2$	Na$_2$O	P$_2$O$_5$	SrO
Content (%)	44.7	27.4	13.1	3.96	3.34	1.19	0.07	1.14	0.52	0.34	0.13	0.07

moisture content, defined as ratio of the mass of water to the mass of solid in the soil. With the known values of bulk density and moisture content, the dry density of the sample was estimated.

The broken soil sample after the UCT test was sieved through a 0.5 mm sieve. About 10 g of soil was taken from sieved soil and subjected to the TCLP test (USE-PA, 1983); another 10 g soil sample was subjected to the SPLP test (solid waste-Extraction Procedure for Leaching Toxicity-Sulphoric Acid & Nitric Acid Method, SPLP) (GB 5085.3-2007). In the TCLP test, sodium acetate was used as an extraction solution, which has pH value of 4.93 ± 0.05 and the solid-to-liquid ratio was 1:20. In the SPLP test, concentrated sulfuric acid and nitric acid mixture was used as extraction solution (mass ratio of sulfuric acid to nitric acid was 2:1), which had pH value of 3.2 ± 0.05 and the solid-to-liquid ratio was 1:20. After the TLCP or SPLP test, the leachate was collected and left to stand for 1 h prior to the pH measurement. The pH was tested using a HORIBA pH/COND METER D-54 pH tester. After the pH test, the leachate was filtered through a 0.45 μm membrane and its supernatant (about 10 mL) was taken. The supernatant was acidized by concentrated nitric acid until its pH value reached less than 2, i.e., pH < 2, and then the concentrations of leached Zn and Pb were measured using a flame atomic absorption spectrophotometer (Thermo Scientific ICE 3000). Triplicates were made and the average values of concentration were recorded.

TEST RESULTS

Change of Moisture Content with Curing Time

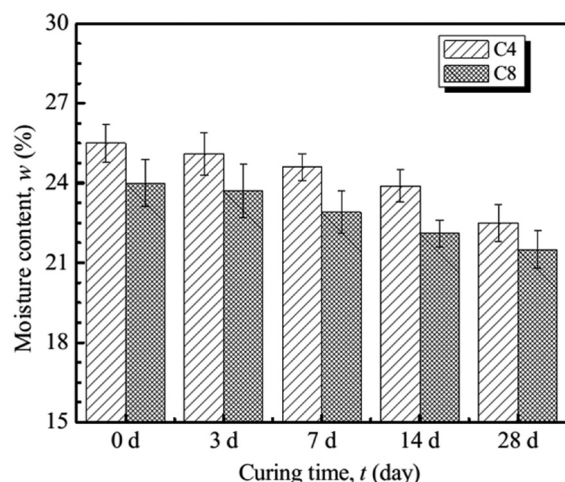Figure 1 presents the variation in the moisture con-

tent with curing time. It can be seen that the moisture content of both C4 and C8 samples tends to decrease as the curing time increases. At a given curing time, the moisture content of C8 sample is about 1.0–1.8% lower than that of C4 sample. For example, at 28 d of curing, the moisture content of C8 sample is about 1% lower than C4 sample; at 14 d of curing, the difference in the moisture content is about 1.8%. When curing time increases from 0 to 28 d, the moisture content of the C4 sample decreases by around 11.7%, and that of C8 does by around 10.4%.

Change of Dry Density with Curing Time

Figure 2 shows the variation in the dry density with the curing time. The dry density of both C4 and C8 soil samples increases with curing time; the increment of the dry density is within 1.21–1.33 g/cm³. The dry density of the C8 sample is often approximately 2% higher than the C4 sample at a given curing time. From 0 to 28 d, the dry density of the C8 sample increases by approximately 16%, and that of C4 sample does by about 13%.

Stress-Strain Correlation

Figure 3 illustrates the stress-strain curves obtained from the UCT. It can be seen that the change in the stress-strain relation with respect to curing time and cement content is consistent with previous study [13]. The samples with longer curing time or higher cement content display greater stress resistance to broken, yet possess lower stress resistance after it reaches the peak, illustrating a strain softening behavior. The stress-strain curves of C4 and C8 samples can be divided
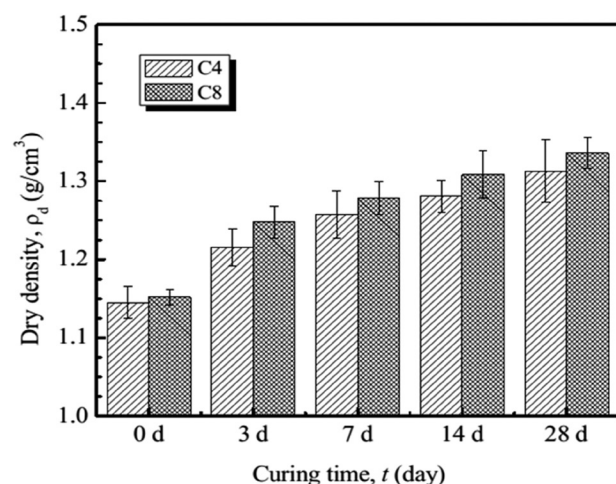

Figure 1. *Change of moisture content with curing time.*

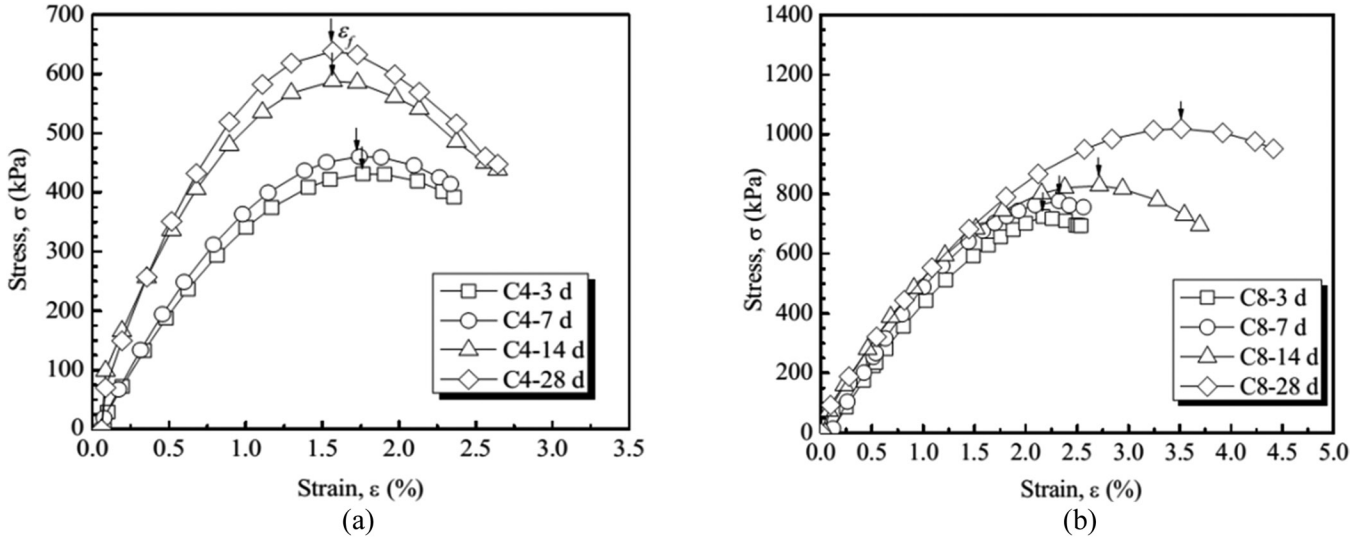**Figure 2.** *Change of dry density with curing time.*

Figure 3. *Stress-strain curve of heavy metal contaminated soils.*

into three stages: elastic deformation stage when the stress and the strain basically exhibit a linear relation; plastic yield stage when the soil experiences nonlinear deformation; and failure stage. As the curing time increases, the peak stress (i.e., q_u) value for both C4 and C8 samples increases as well. For example, the peak stress of C4 sample at 14 d of curing is significantly higher relative to 7 d of curing; the peak stress of C8 sample at 28 d of curing is noticeably higher relative to 14 d of curing. The peak stress value of the C8 sample is often higher than that of the C4 sample, regardless of the curing time.

Change of UCS with Curing Time

Figure 4 illustrates the variation in q_u with the curing time. The q_u of cement solidified soil is much greater than that of untreated contaminated soil throughout the 28 d of curing (Figure 4). Moreover, the q_u of the C8 sample is approximately 1.6 times that of the C4 sample. The q_u of C4 and C8 samples at 28 d of curing increases by 48% and 31.6%, respectively, as compared to the 3 d of curing. The q_u of both C4 and C8 samples is remarkably greater than that of the untreated soil, illustrating a higher bonding strength of the soils admixed with cement additives.

Correlation Between Strength and Secant Modulus

The secant modulus (E_{50}) is defined as the ratio of compressive stress to its corresponding strain ε, and is expressed by:

$$E_{50} = \sigma_{1/2} \Big/ \frac{1}{2}\varepsilon_f \tag{1}$$

where $\sigma_{1/2}$ is the stress when the strain is equal to half of the strain at failure (ε_f).

It has been shown that q_u has a linear relation with E_{50} for the cement solidified soil, and the relation can be expressed by:

$$E_{50} = \eta \cdot q_u \tag{2}$$

where η is a dimensionless constant.

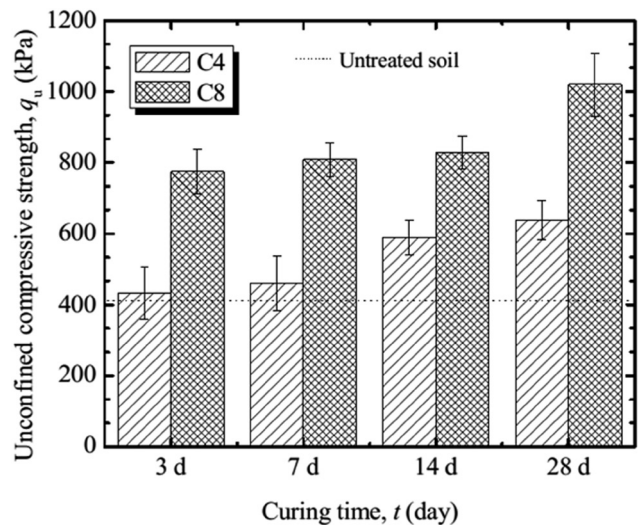Figure 5 presents the relation between E_{50} and q_u for the C4 and C8 samples at curing times of 3, 7, 14 and

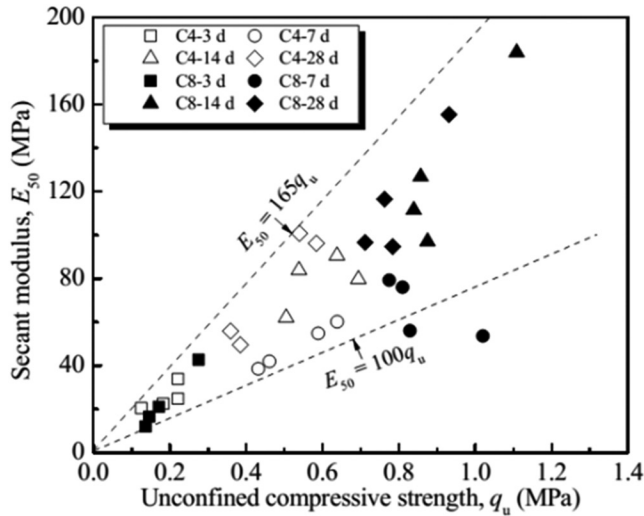**Figure 4.** *Change of q_u with curing time.*

Figure 5. *Correlation between secant modulus and UCS.*

28 d. The η value obtained in this study ranges from 100 to 165, which is very close to the result for cement-solidified Zn-contaminated soil reported by [14].

Change of Leachate pH with Curing Time

Figure 6 shows the variation in the leachate pH with the curing time. It can be seen that the pH values in both TCLP and SPLP tests tend to decrease with increasing curing time. In the TCLP test, the leachate pH of the C4 and C8 samples at 28 d of curing decreases by 1.19–1.23, as compared to the pH value at 0 d of curing. A drastic decrease in leachate pH is observed at 3 d of curing in both C4 and C8 samples. The change in pH with respect to curing time is insignificant for both
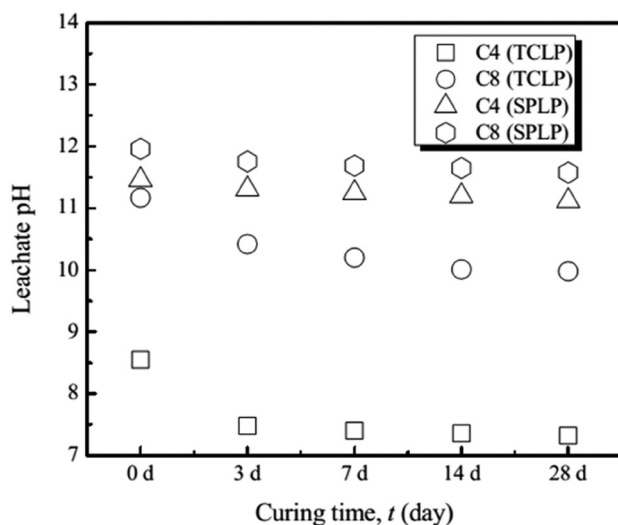
C4 and C8 samples after 3 d of curing. In the SPLP test, the leachate pH values for C4 and C8 samples at 28 d of curing are lower (0.34–0.38 unit) than their values at 0 d. At 28 d curing, the TCLP leachate pH value for the C8 sample is significantly higher than the C4 sample by 2.3 units; however, this difference is only 0.36 unit in the case of SPLP test. Due to different extraction solutions used in the TCLP and SPLP tests, the leachate pH of the former is often lower than that of the latter.

Change of Pb and Zn Concentrations in Leachate with Curing Time

Figure 7 shows the variation in the leached Pb and Zn concentration with the curing time, obtained from the TCLP tests. It can be seen from Figure 7 that both Pb and Zn concentrations decrease gradually with curing time. At 14 d of curing, Pb concentration reaches the lowest value (0.005 mg/L); whereas the Zn concentration decreases continuously with the curing time. Within the 28 d of curing, the Zn concentration of the C8 sample is often lower relative to the C4 sample; nevertheless, the difference in the leached Pb concentration between the C4 and C8 samples is marginal. At 28 d of curing, the Pb and Zn concentrations of C8 samples meet the environmental regulatory limits for class-II surface water (GB3838-2002), and Pb and Zn concentrations of C4 samples meet the the environmental regulatory limits for class-III and class-II surface water (GB3838-2002), respectively.

Figure 8 shows the variation in the leached Pb and Zn concentration with the curing time, obtained from the SPLP tests. The Pb and Zn concentrations decrease
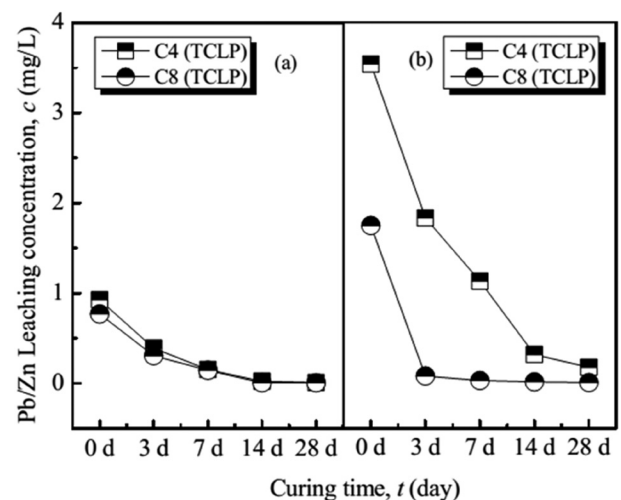

Figure 6. *Change of leachate pH with curing time.*

Figure 7. *TCLP test results showing the variation in the leached. Pb/Zn concentration with the curing time: (a) Pb and (b) Zn.*

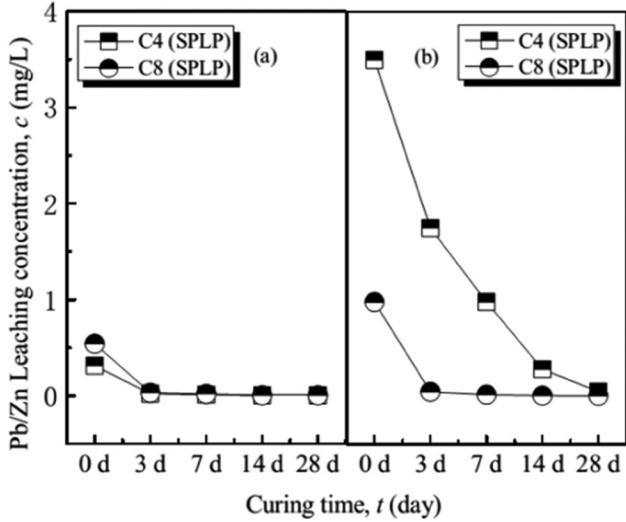**Figure 8.** *SPLP test results showing the variation in the leached.*

Figure 9. *Relationship between q_u and leached Zn concentration. Pb/Zn concentration with the curing time curve: (a) Pb and (b) Zn.*

with increasing curing time. The leached Zn concentration of the C8 samples is always lower than that of the C4 sample; the Pb concentration of the C8 samples is almost the same as that of the C4 sample from 3 d of curing. After 28 d of curing, the Pb and Zn concentrations of C8 and C4 samples meet the the environmental regulatory limits of class-II surface water (GB3838-2002).

A regress analysis is conducted for identifying the correlation between q_u and leached Zn concentrations using the least-square-root method. The derived equation is expressed by:

$$q_u/q_{u,3d} = \frac{1}{1.24 \times 5.9 \cdot c_t/c_{3d}} + 0.86, R^2 = 0.94 \quad (3)$$

where $q_{u,t}$ denotes q_u at a curing time of t d; $q_{u,3d}$ denotes the q_u at 3 d of curing; c_t denotes the leached Zn concentration at curing time of t d; c_3 denotes the leached Zn concentration at 3 d of curing. More data is warranted to validate the general applicability of the proposed Equation 3.

Change of Immobilization Percentage with Curing Time

In this study, the parameter immobilization percentage (*IP*) was introduced to evaluate the effectiveness of the cement-based solidification/stabilization, and it is defined by the following equation:

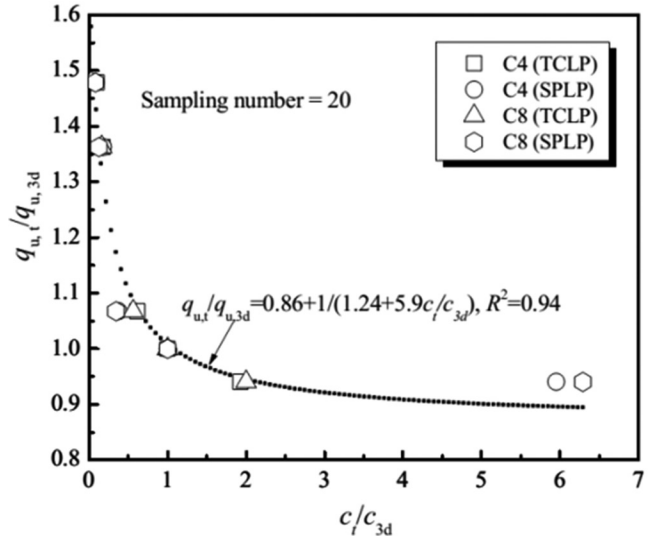$$IP = \frac{C_0 - C_1}{C_0} \times 100\% \quad (4)$$

where C_0 refers to the concentration of Pb or Zn of untreated contaminated soil; C_1 refers to the concentration of Pb or Zn of solidified soil at a given curing time.

Figures 10 and 11 illustrate the variation in *IP* for Pb and Zn with the curing time in the case of TCLP and SPLP tests, respectively. It can be seen that *IP* of Pb or Zn increases with increasing curing time. The TCLP test results show that at 3 d of curing, the *IP*s of Pb and Zn of the C8 samples are 60% and 50%, respectively, which are only 1.8–2.7% higher than those of C4 samples. After 14 d of curing, the *IP*s of Pb and Zn of C8 and C4 samples basically stabilize over 90%. The *IP*s of Pb and Zn of C8 samples are often higher than those of C4 samples. In addition, the *IP* of Pb is higher than that of Zn for the same cement content and curing time.
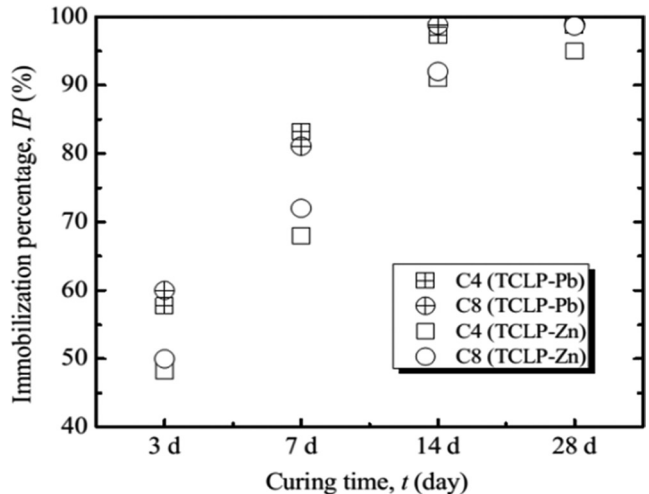

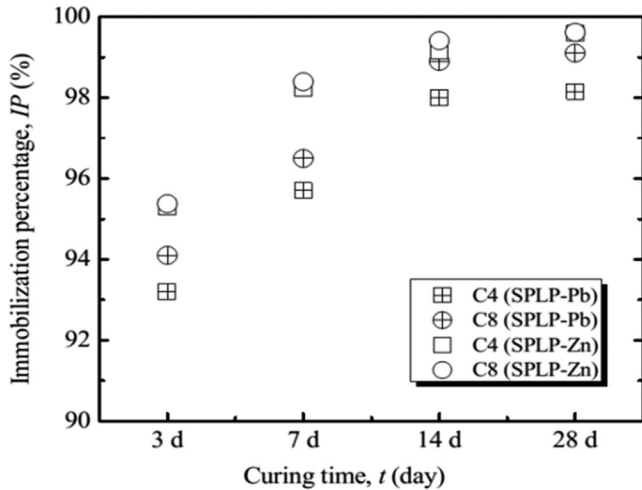**Figure 10.** *Immobilization percentage relative to curing time (TCLP).*

Figure 11. *Immobilization percentage relative to curing time (SPLP).*

The SPLP test results show that the *IP*s of Pb and Zn obtained by this method are generally higher than those by the TCLP method. At 3 d of curing, the *IP*s of Pb and Zn both exceed 92% and the *IP*s of Pb and Zn increase to some extent with the increase in curing time. Evidently, the SPLP test results are more conservative as compared to the TCLP test results.

DISCUSSIONS

The results demonstrate that the strength and leachability of the contaminated soils are significantly affected by the curing time and cement content. The observations are attributed to the cement hydration and pozzolanic reactions occurred in the cement solidified soils [15]. As the curing time increases, the two ongoing reactions consume pore water in the soils, generating calcium silicate hydrate (CSH), ettringite (AFt) and other hydration products. As a result, pores in the solidified soil are filled by hydration products, causing a reduction in moisture content and an increase in dry density with respect to curing time. The hydration and pozzolanic reactions become more intense with the elevated cement content, making the moisture content (dry density) of the C8 sample lower (higher) than that of C4 sample. The CSH, AFt and other hydration products formed in the soils can enhance their strengths [15]. Generally, the quantity of these hydration products increases with increasing cement content. As a result, the unconfined compressive strength of the C8 sample is higher than that of the C4 sample.

The immobilizations of Pb and Zn with cement or cement-based materials are attributed to the surface sorption of CSH, precipitations of Pb and Zn hydrox-

ides, and entry of these hydroxides into the CSH crystal lattices by substitution [16]. The quantity of hydration products in the samples increases with increasing curing time; therefore, the immobilization degrees of Pb and Zn increase while the leached Pb or Zn concentration decreases with increasing curing time. The higher immobilization percentage of the C8 sample relative to C4 sample is attributed to the more intense hydration and pozzolanic reactions in the former case. Since the pozzolanic reaction of cement continuously consumes OH$^-$ through the entire curing time, the pH of the leachate decreases with the increase in the curing time. The increase in cement content can also lead to intensified alkalinity in the sample, which is why the leachate pH of the C8 sample is higher than that of the C4 sample. In addition, as sodium acetate solution used in the TCLP test has better buffering capacity than sulfuric acid-nitric acid mixed solution used in the SPLP test, the leached Pb or Zn concentration in the former test is higher than that in the latter.

CONCLUSIONS

This study addresses the issue of heavy metal contaminated soil treatment in the Hunan Province. Laboratory tests were conducted to investigate the strength and leaching characteristics of cement solidified Pb- and Zn-contaminated soil. The following conclusions are drawn based on this study:

1. The water in the soil was consumed during hydration with increasing curing time, which was responsible for the reduced moisture content and increased dry density. After 28 d of curing, the moisture content of the C8 sample was 1–1.8% lower than that of the C4 sample, and the dry density of the C8 sample was 3.4% higher than that of the C4 sample.

2. The unconfined compressive strength of the cement solidified soil was much higher than that of the untreated soil. The unconfined compressive strength of the C8 sample was often higher than that of the C4 sample.

3. A linear correlation between the unconfined compressive strength (q_u) and secant modulus (E_{50}) was proposed and it was expressed by $E_{50} = (100 - 165)q_u$, which is consistent with previous studies.

4. The leachate pH of both the TCLP test and the SPLP test decreased with increasing curing time; pH of the former was lower than that of the latter, irrespective of the curing time or cement content. The leachate pH obtained in the TCLP test and the SPLP

test dropped by 1.19–1.23 and 0.34–0.38 units, respectively, when the curing time increased from 0 to 28 d.

5. Leached Pb and Zn concentrations for both TCLP and SPLP tests decreased steadily with the curing time. In addition, the leached concentration of Zn for the C8 sample was often lower than that for the C4 sample, yet their Pb concentrations stayed close to each other.

6. The immobilization percentage of Pb and Zn in both TCLP and SPLP tests increased as curing time increased. By the end of the 28 d of curing, the leached concentrations of Pb and Zn of the cement solidified soils meet the China environmental regulatory limits for class-III or class-II surface water.

7. A simplified empirical equation is proposed for predicting the strength of the cement treated contaminated soil.

ACKNOWLEDGEMENTS

REFERENCES

1. LI Xiao-hu. The mine environmental pollution and remediation in large metal mines. Lanzhou: Lanzhou University, 2007. (in Chinese)

2. ZHONG Shun-qing. Soil contamination and remediation in the diggings area. *Resource Development & Market,* 2007, 06:532–534. (in Chinese)

3. DAS S, PATNAIK S C,SAHU H K, CHAKRABORTY A, SUDAR-SHAN M, THATOI H N. Heavy metal contamination, physico-chemical and microbial evaluation of water samples collected from chromite mine environment of Sukinda, India. *Trans. Nonferrous Met. Soc. China,* 2013, 23(2): 484–493.

4. BURDEN F R, DONNERT D, GODISH T, MCKELVIE I D. Environmental monitoring handbook. Boston: The McGraw-Hill Companies, 2004.

5. EVANKO C R, DZOMBAK D A. Remediation of metals-contaminated soils and groundwater technology. Pittsburgh, PA: Carnegie Mellon University, 1997.

6. ZHU Wei, LI Lei, LIN Cheng. Biochemical effects on permeability of solidified sludge. *Rock and Soil Mechanics,* 2006, 27(6): 933–938. (in Chinese)

7. LIU Yun-guo, LI Xin, ZENG Guang-ming, HUANG Bao-rong, ZHANG Hui-zhi. Electrokinetics removal of lead from lead-contaminated red soils. *Trans. Nonferrous Met. Soc. China,* 2003, 13(6): 1003–6326.

8. ANON. Improved cement solidification of low and intermediate level radioactive wastes. Vienna, Austria: International Atomic Energy Agency, 1993.

9. TERASHI M H, TANAKA H, MITSUMOTO T, NIIDOME Y, HONMA S. Fundamental properties of lime and cement treated soils (2nd report). Yokosuka: Report of the Pore and Harbour Research Institute, 1980. (in Japanese)

10. MINOCHA A K, JAIN N, VERMA C L. Effect of inorganic materials on the solidification of heavy metal sludge. *Cement and Concrete Research,* 2003, 33(10):1695–1701.

11. LEE D. Formation of leadhillite and calcium lead silicate hydrate (C-Pb-S-H) in the solidification/stabilization of lead contaminants. *Chemosphere,* 2007, 66(9):1727–1733.

12. STEPANOVA I N, LUKINA L G, SVATOVSKAYA L B, SYCHEV M M. Hardening of cement pastes in presence of chloride of 3d elements. *Journal of Applied Chemistry of the USSR,* 1981, 54(5): 885–888.

13. DU Y J, WEI M L, JIN F, LIU Z B. Stress-strain relation and strength characteristics of cement treated zinc-contaminated clay. *Engng Geol,* 2013, 167: 20–26.

14. DU Y J, JIANG N J, LIU S U, JIN F, SINGH D N, PUPPALA A J. Engineering properties and microstructural characteristics of cement-stabilized zinc-contaminated kaolin. *Canadian Geotechnical Journal,* 2014, 51(3): 289–302.

15. DU Yan-jun, JIANG Ning-jun, WANG Le, WEI Ming-li. Strength and microstructure characteristics of cement-based solidified/stabilized zinc-contaminated kaolin. *Chinese Journal of Geotechnical Engineering,* 2012, 11:2114–2120. (in Chinese)

16. GOUGAR M L D, SCHEETZ B E, ROY D M. Ettringite and C-S-H Portland cement phases for waste ion immobilization: a review. *Waste Management,* 1996, 16(4): 295–303.

GUIDE TO AUTHORS

1. Manuscripts shall be sent electronically to the Editor-in-Chief, Dr. P. Brent Duncan at pduncan@unt.edu using Microsoft Word in an IBM/PC format. If electronic submission is not possible, three paper copies of double-spaced manuscripts may be sent to Dr. P. Brent Duncan, (Editor of the *Journal of Residuals Science & Technology,* University of North Texas, Biology Building, Rm 210, 1510 Chestnut St., Denton, TX 76203-5017) (Tel: 940-565-4350). Manuscripts should normally be limited to the space equivalent of 6,000 words. The editormay waive this requirement in special occasions. As a guideline, each page of a double-spaced manuscript contains about 300 words. Include on the title page the names, affiliations, and addresses of all the authors, and identify one author as the corresponding author. Because communication between the editor and the authors will be electronic, the email address of the corresponding author is required. Papers under review, accepted for publication, or published elsewhere in journals are normally not accepted for publication in the *Journal of Residuals Science & Technology*. Papers published as proceedings of conferences are welcomed.

2. Article titles should be brief, followed by the author's name(s), affiliation, address, country, and postal code (zip) of author(s). Indicate to whom correspondence and proofs should be sent, including telephone and fax numbers and e-mail address.

3. Include a 100-word or less abstract and at least six keywords.

4. If electronic art files are not supplied, submit three copies of camera-ready drawings and glossy photographs. Drawings should be uniformly sized, if possible, planned for 50% reduction. Art that is sent electronically should be saved in either a .tif or .JPEG files for superior reproduction. All illustrations of any kind must be numbered and mentioned in the text. Captions for illustrations should all be typed on a separate sheet(s) and should be understandable without reference to the text.

5. DEStech uses a numbered reference system consisting of two elements: a numbered list of all references and (in the text itself) numbers in brackets that correspond to the list. At the end of your article, please supply a numbered list of all references (books, journals, web sites etc.). References on the list should be in the form given below. In the text write the number in brackets corresponding to the reference on the list. Place the number in brackets inside the final period of the sentence cited by the reference. Here is an example [2].

   Journal: 1. Halpin, J. C., "article title", *J. Cellular Plastics,* Vol. 3, No. 2, 1997, pp. 432–435.

   Book: 2. Kececioglu, D. B. and F.-B. Sun. 2002. *Burn-In Testing: Its Quantification and Optimization,* Lancaster, PA: DEStech Publications, Inc.

6. Tables. Number consecutively and insert closest to where firstmentioned in text or type on a numbered, separate page. Please use Arabic numerals and supply a heading. Column headings should be explanatory and carry units. (See example at right.)

7. Units & Abbreviations. Metric units are preferred. English units or other equivalents should appear in parentheses if necessary.

8. Symbols. A list of symbols used and their meanings should be included.

Table 5. Comparison of state-of-the-art matrix resins with VPSP/BMI copolymers.

Resin System	Core Temp. (DSC peak)	T_E	Char Yield, %
Epoxy (MY720)	235	250	30
Bismaleimide (H795)	282	>400	48
VPSP/Bismaleimide copolymer			
C379: H795 = 1.9	245	>400	50
C379: H795 = 1.4	285	>400	53

9. Page proofs. Authors will receive page proofs by E-mail. Proof pages will be in a .PDF file, which can be read by Acrobat Reader. Corrections on proof pages should be limited to the correction of errors. Authors should print out pages that require corrections and mark the corrections on the printed pages. Pages with corrections should be returned by FAX (717-509-6100) or mail to the publisher (DEStech Publications, Inc., 439 North Duke Street, Lancaster, PA 17602, USA). If authors cannot handle proofs in a .PDF file format, please notify the Editor, Dr. P. Brent Duncan at pduncan@unt.edu.

10. Index terms.With proof pages authors will receive a form for listing key words that will appear in the index. Please fill out this form with index terms and return it.

11. Copyright Information. All original journal articles are copyrighted in the name of DEStech Publications, Inc. All original articles accepted for publication must be accompanied by a signed copyright transfer agreement available from the journal editor. Previously copyrighted material used in an article can be published with the *written* permission of the copyright holder (see #14 below).

12. Headings. Your article should be structured with unnumbered headings. Normally two headings are used as follows:

    Main Subhead: DESIGN OF A MICROWAVE INSTALLATION Secondary Subhead: Principle of the Design Method

    If further subordination is required, please limit to no more than one (*Third Subhead*).

13. Equations. Number equations with Arabic numbers enclosed in parentheses at the right-hand margin. Type superscripts and subscripts clearly above or below the baseline, or mark them with a caret. Be sure that all symbols, letters, and numbers are distinguishable (e.g., "oh" or zero, one or lowercase "el," "vee" or Greek nu).

14. Permissions. The author of a paper is responsible for obtaining releases for the use of copyrighted figures, tables, or excerpts longer than 200 words used in his/her paper. Copyright releases are permissions to reprint previously copyrighted material. Releases must be obtained from the copyright holder, which is usually a publisher. Forms for copyright release will be sent by the editor to authors on request.

General: The *Journal of Residuals Science & Technology* and DEStech Publications, Inc. are not responsible for the views expressed by individual contributors in articles published in the journal.

DEStech Publications, Inc.

439 NORTH DUKE STREET
LANCASTER, PENNSYLVANIA 17602-4967, U.S.A.

www.destechpub.com